Follow up studies of Planck Cold Dust Clumps

Yuefang Wu

Astronomy Department
Peking University

Outline

- Early phase of star formation and samples
- Results of Planck Satellite
- Herschel studies
- Millimeter line observations
- Summary and future work

Early phase of star formation (SF) and samples

Characteristics of SF early phase: --difficult to obtain

--still in looking for

Large samples are the key

Since last 70',

- Optical selection:

  Shapless HII regions

  (Dickinson et al. 1974; Evans et al. 1977) Td >30 K

  Nearby dark clouds from PSS:

  13CO Ta*: 5-15 K (Myers et al. 1983)

- IRAS sources UC HII gas ionized (Wood & Churchwell 1989)
- Infrared dark clouds (Egan et al. 1998) :Tbol< 20 K

  Near Galactic plane: b: ±6o

- IRAC, MIPS provide large amount of infrared sources

  Not "early" or "large" enough, even low mass starless cores – embedded low-luminosity protostar (Schnee et al. 2012)

THE ASTROPHYSICAL JOURNAL, **217**: 448–463, 1977 October 15

THE ENERGETICS OF MOLECULAR CLOUDS. I. METHODS OF ANALYSIS AND APPLICATION TO THE S255 MOLECULAR CLOUD

N. J. EVANS II*†
Department of Astronomy and McDonald Observatory, University of Texas at Austin
GUY N. BLAIR†
Department of Astronomy and McDonald Observatory, University of Texas at Austin, and Netherlands Foundation for Radio Astronomy
S. BECKWITH
Department of Physics, California Institute of Technology
Received 1977 February 24; accepted 1977 April 7

Early results of Planck Satellite

Now Planck dust clumps:

-- All sky survey

-- Submm-mm emission

-- Multiple bands

Observations:

Two instruments:

- Low Frequency Instrument (LFI)

  covering three bands centred at 30, 44, and 70 GHz

- High Frequency Instrument (HFI)

Covering six bands centred at 100, 143, 217, 353, 545 and 857 GHz.

Results:

Planck team: more 30 papers from 2011

Planck Early Results: The Galactic Cold Core Population revealed by the first all-sky survey

Planck Collaboration: P. A. R. Ade, N. Aghanim, M. Arnaud, M. Ashdown, J. Aumont, C. Baccigalupi, A. Balbi,
A. J. Banday, R. B. Barreiro, J. G. Bartlett, E. Battaner, K. Benabed, A. Benoît, J.-P. Bernard, M. Bersanelli, R. Bhatia,
[illegible]

Planck Early Results: All sky temperature and dust optical depth from *Planck* and *IRAS*: Constraints on the "dark gas" in our Galaxy

Planck Collaboration: P. A. R. Ade, N. Aghanim, M. Arnaud, M. Ashdown, J. Aumont, C. Baccigalupi, A. Balbi,
A. J. Banday, R. B. Barreiro, J. G. Bartlett, E. Battaner, K. Benabed, A. Benoît, J.-P. Bernard, M. Bersanelli, R. Bhatia,
[illegible]

Planck Early Results: Dust in the diffuse interstellar medium and the Galactic halo

Planck Collaboration: A. Abergel, P. A. R. Ade, N. Aghanim, M. Arnaud, M. Ashdown, J. Aumont, C. Baccigalupi, A. Balbi,
A. J. Banday, R. B. Barreiro, J. G. Bartlett, E. Battaner, K. Benabed, A. Benoît, J.-P. Bernard, M. Bersanelli, R. Bhatia,
K. Blagrave, J. J. Bock, A. Bonaldi, J. R. Bond, J. Borrill, F. R. Bouchet, F. Boulanger, M. Bucher, C. Burigana, P. Cabella,
C. M. Cantalupo, J.-F. Cardoso, A. Catalano, L. Cayón, A. Challinor, A. Chamballu, L.-Y Chiang, C. Chiang,
P. R. Christensen, D. L. Clements, S. Colombi, F. Couchot, A. Coulais, B. P. Crill, F. Cuttaia, L. Danese, R. D. Davies,
R. J. Davis, P. de Bernardis, G. de Gasperis, A. de Rosa, G. de Zotti, J. Delabrouille, J.-M. Delouis, F.-X. Désert, C. Dickinson,
S. Donzelli, O. Doré, U. Dörl, M. Douspis, X. Dupac, G. Efstathiou, T. A. Enßlin, H. K. Eriksen, F. Finelli, O. Forni,
M. Frailis, E. Franceschi, S. Galeotta, K. Ganga, M. Giard, G. Giardino, Y. Giraud-Héraud, J. González-Nuevo,
K. M. Górski, S. Gratton, A. Gregorio, A. Gruppuso, F. K. Hansen, D. Harrison, G. Helou, S. Henrot-Versillé, D. Herranz,
S. R. Hildebrandt, E. Hivon, M. Hobson, W. A. Holmes, W. Hovest, R. J. Hoyland, K. M. Huffenberger, A. H. Jaffe,
G. Joncas, A. Jones, W. C. Jones, M. Juvela, E. Keihänen, R. Keskitalo, T. S. Kisner, R. Kneissl, L. Knox,
H. Kurki-Suonio, G. Lagache, J.-M. Lamarre, A. Lasenby, R. J. Laureijs, C. R. Lawrence, S. Leach, R. Leonardi,
C. Leroy, M. Linden-Vørnle, F. J. Lockman, M. López-Caniego, P. M. Lubin, J. F. Macías-Pérez, C. J. MacTavish, B. Maffei,
D. Maino, N. Mandolesi, R. Mann, M. Maris, D. J. Marshall, P. Martin, E. Martínez-González, S. Masi, S. Matarrese,
F. Matthai, P. Mazzotta, P. McGehee, P. R. Meinhold, A. Melchiorri, L. Mendes, A. Mennella, M.-A. Miville-Deschênes,
A. Moneti, L. Montier, G. Morgante, D. Mortlock, D. Munshi, A. Murphy, P. Naselsky, F. Nati, P. Natoli,
C. B. Netterfield, H. U. Nørgaard-Nielsen, F. Noviello, D. Novikov, I. Novikov, I. J. O'Dwyer, S. Osborne, F. Pajot, R. Paladini,
F. Pasian, G. Patanchon, O. Perdereau, L. Perotto, F. Perrotta, F. Piacentini, M. Piat, D. Pinheiro Gonçalves, S. Plaszczynski,
[illegible]

Public released Early results:

- The Cold Core Catalogue of Planck Objects (C3PO)

  10783

  → The first unbiased all-sky catalogue

- The Early Cold Core Catalogue (ECC)

  Temperature, mass, morphology

  915 are the most reliable

  T_d: 7—17 K

  β: 1.4 –2.8

  D: < 2 kpc   few at 4 kpc

  Mass 1-10^5 Msun

Herschel studies:

- Aim: drive physical properties for
  Planck full cold clump population
  --Herschel Science Demonstration Phase
- 150 target fields will be observed with PACS and SPIRE:
- Mapping with multiple wavelengths
- So far 74 fields were observed
  Juvela et al. 2010, 2011, 2012

The three fields first observed as part of the Herschel SDP

--first glimpse into the nature of these sources.

Target	RA (J2000)	Dec (J2000)	Map size (PACS/SPIRE)
PCC 249	22 21 17.6	+63 42 25	50′/50′
PCC 288	22 53 31.3	+62 31 44	18′/30′
PCC 550	12 25 16.5	−71 46 03	18′/30′

R/G/B: 350/260/160 bμm PCC550 : 350/250/160 μm Others

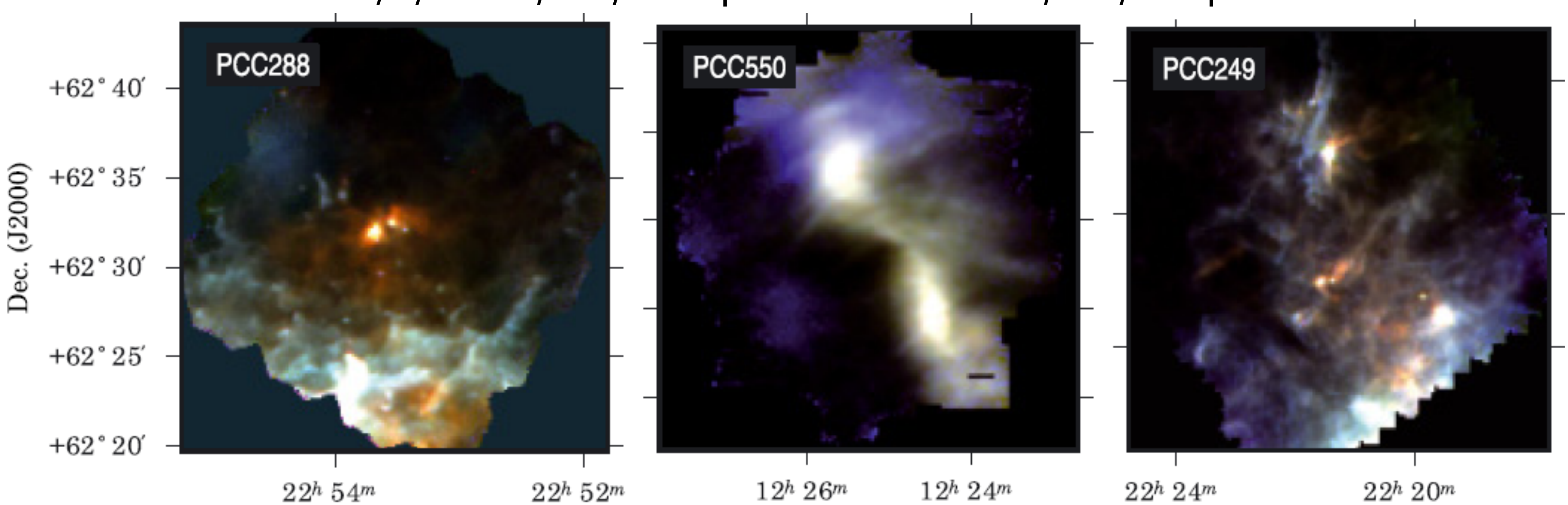

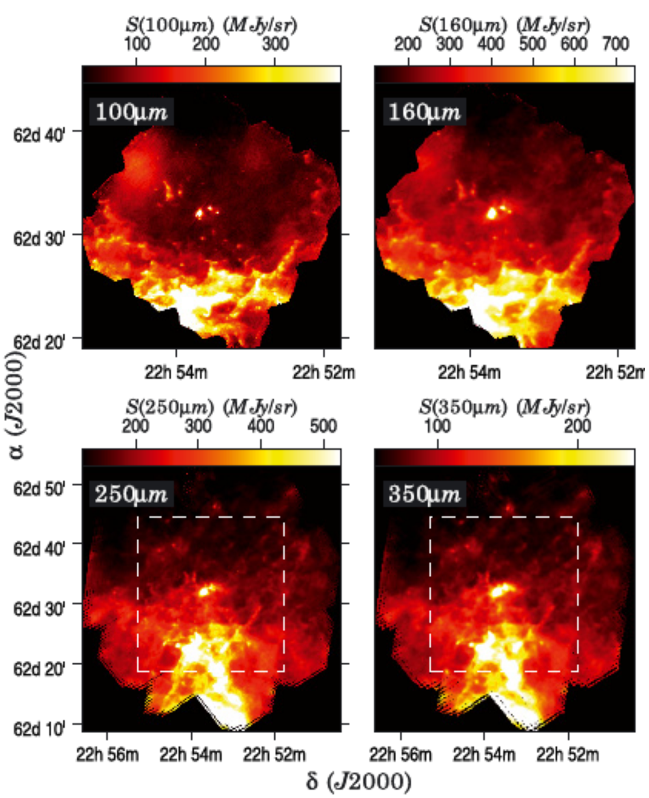

100µm
160µm
250µm
350µm
S(100µm) (MJy/sr)
S(160µm) (MJy/sr)
S(250µm) (MJy/sr)
S(350µm) (MJy/sr)
α (J2000)
δ (J2000)

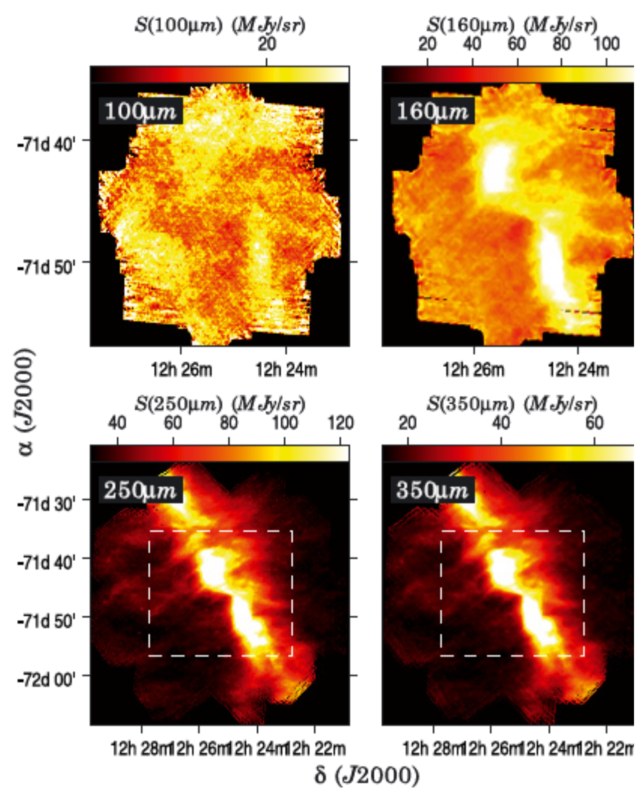

100µm
160µm
250µm
350µm
S(100µm) (MJy/sr)
S(160µm) (MJy/sr)
S(250µm) (MJy/sr)
S(350µm) (MJy/sr)
α (J2000)
δ (J2000)

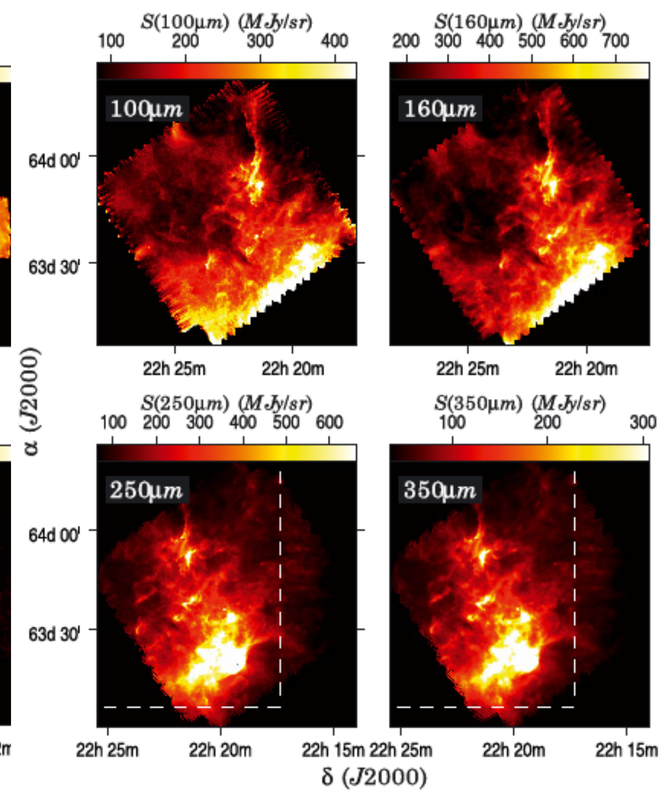

100µm
160µm
250µm
350µm
S(100µm) (MJy/sr)
S(160µm) (MJy/sr)
S(250µm) (MJy/sr)
S(350µm) (MJy/sr)
α (J2000)
δ (J2000)

Colour temperature:

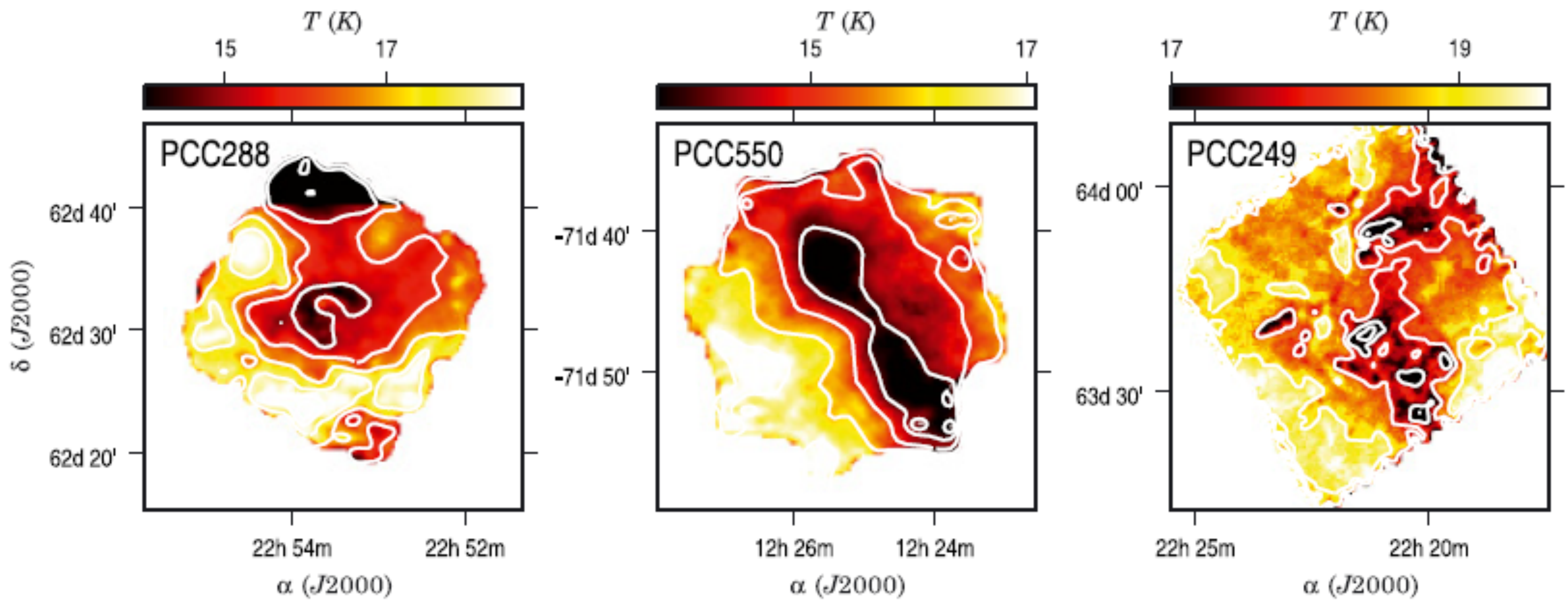

Dust colour temperature maps for the three SDP fields. The calculations assume a fixed value of the spectral index, $\beta = 2.0$. The map resolution is $\sim$37″ and the contours are drawn one Kelvin apart.

Column density:

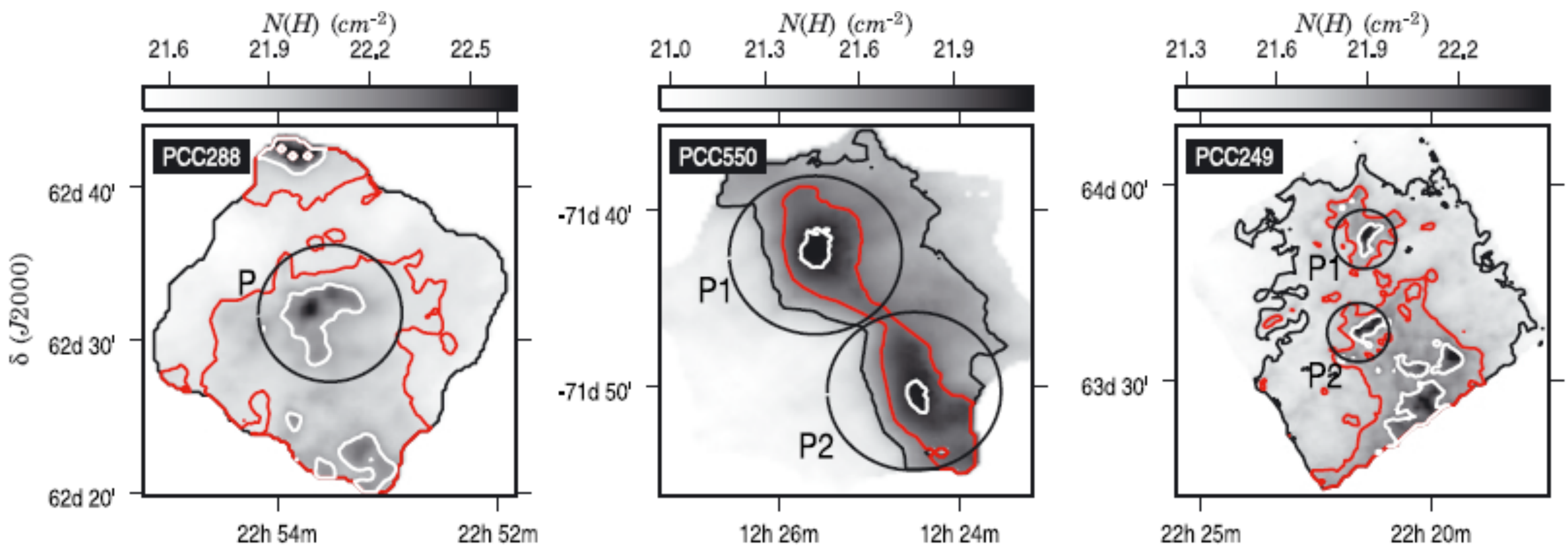

Maps of the hydrogen column density N(H) derived with the colour temperature maps. The maps have a resolution of ~37″ and the contours are drawn at levels where log10 N(H) equals 21.5, 21.8, and 22.1.

- Mass estimated for the three fiels:
- PCC 288 D: 800 pc ~890 Msun
- PCC 550 225 pc ~31
- PCC 249 800 pc ~3800

- So far physical parameter of 74 fields are obtained
  Also obtained their various morphologies
  Coreshine was also detected.

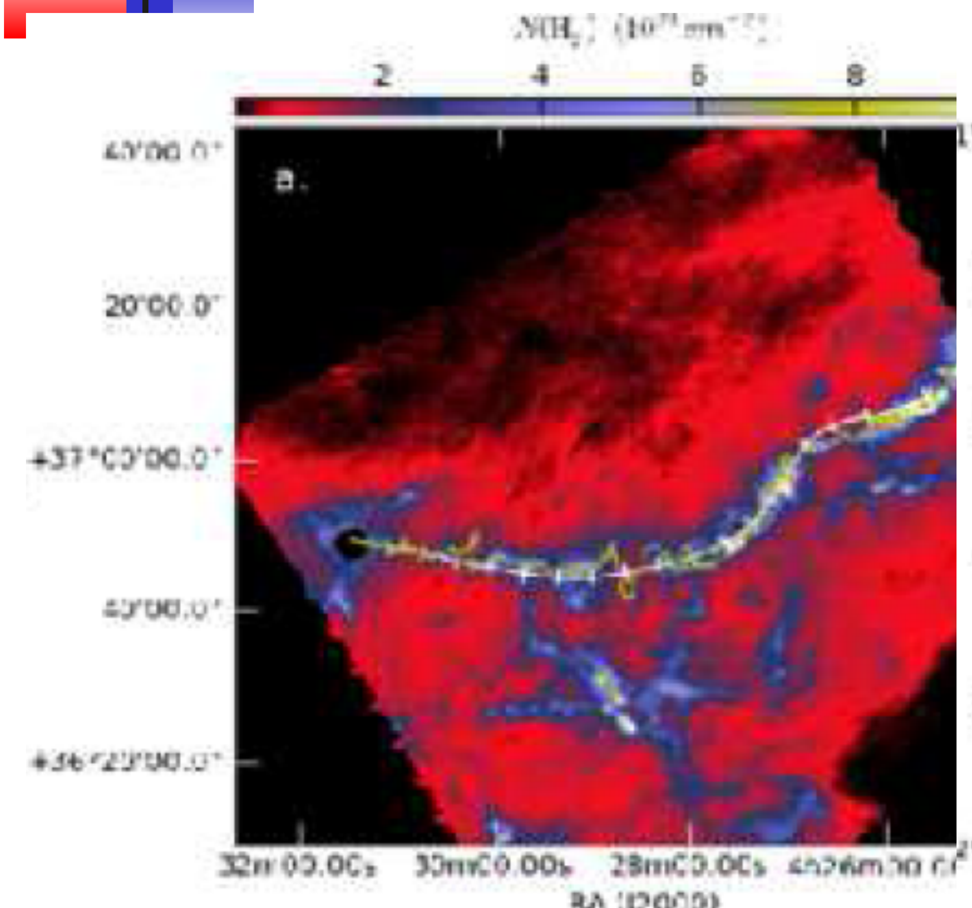

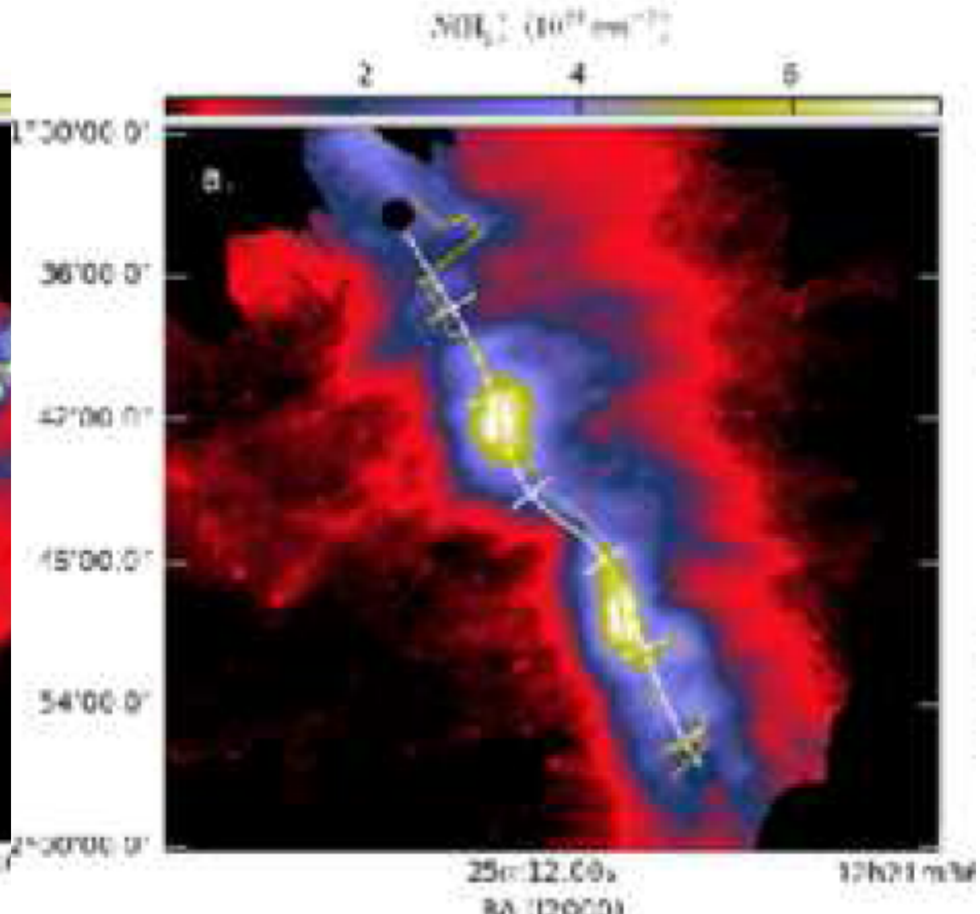

G163.82-8.44
9.00

G300.86-

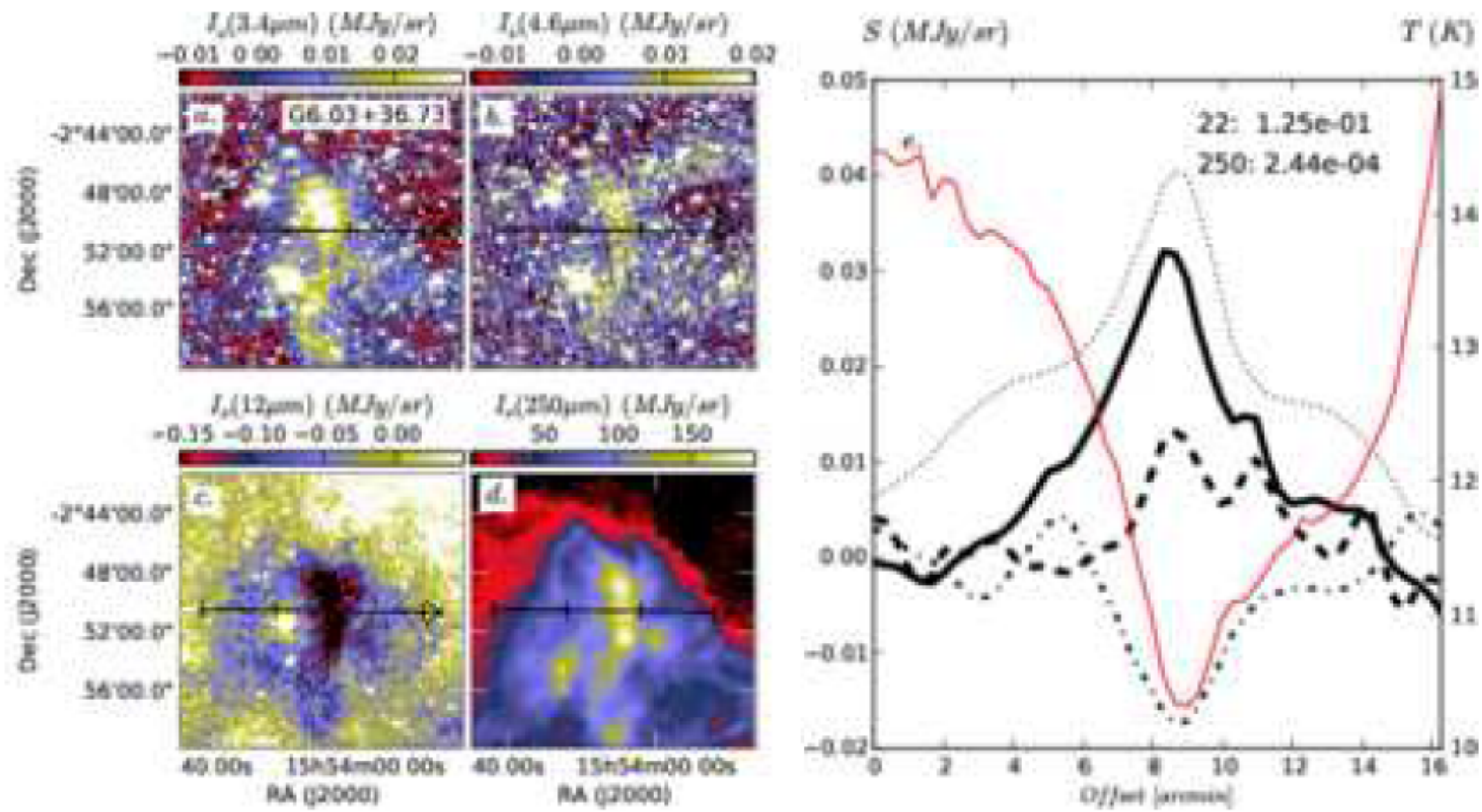

G6.03+0.73 (L183) Wise: 3.4, 4.6, 12 and Spine 250μmbbbbbb

Results of Herschel SDP:

- Distance: 0.1-several kpc
- The colour temperature maps confirm the *Planck detections* of cold dust. The analysis of the total intensity leads to minimum colour temperature of 12−18K in the three fields
- Mass: <10 – 10^4 Msun
- Morphology: Filamentary: >50%   width: 0.2-0.3 pc
  - Cometary
  - Isolated
  - Complex
- Star formation: 20% associated with YSOs
- Coreshine: among 44 sources 4 identified   6 : possible
- à Confirm the capability of the Planck all sky survey for making a large number of new cold core detections

More fields are in investigated: by Juvela (Private communication)
39 have Herschel + Qinghai CO (going to be talked)

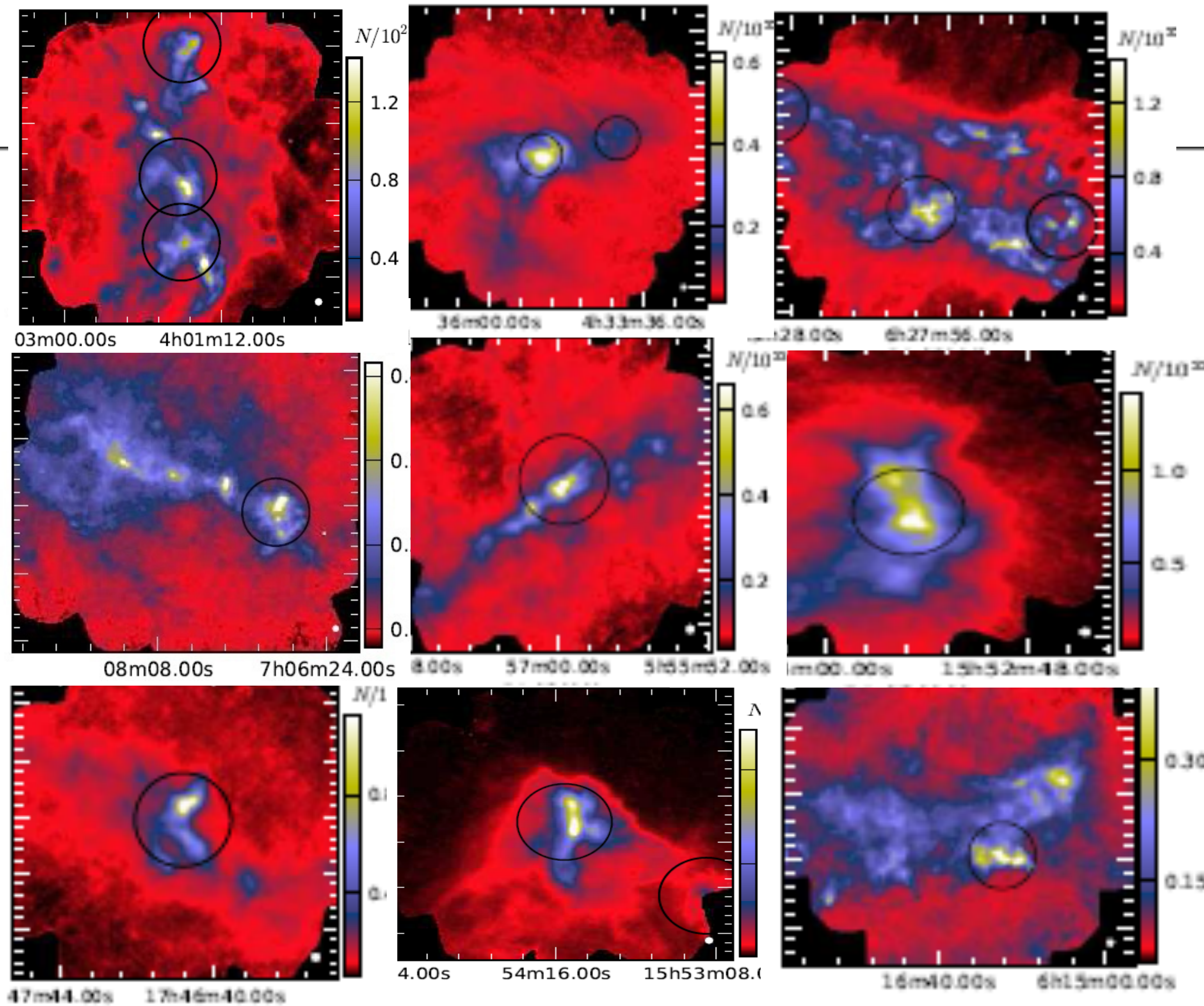

Millimeter line observations

- Gas study: important:

  Gas ~99%;

  All dynamic information- lines

  Planck survey: Cold dust,

  Herschel, still continuum so far

- Ground based line observations:

  IRAM, Effelsberg 100 m, CSO, …

  Our work began when the data were public released:

  ECC cores: Dec. >-20o ; 674

  More than 400 were mapped

Observation

- Purple Mountain Observatory, Qinghai Sation, 13.7m
  same with the one of FCRAO, bu at a higher (3200 m) site
  Observed during Jan. to May of 2011:
- Receiver： Nine beam SIS array
  J=1-0 of 12CO, 13CO，C18O observed at the same time
  HPBW: 56”
- Spectrometer：1GHz/16384 channels
  Velocity resolution: 12CO: 0.16 km/s 13CO, C18O: 0.17 km/s
  rms: 12CO, 0.2 K : 13CO, C18O : 0.1 K
- Observation model： single point: on/off Mapping: OTF

B1950
J2000

Known molecular Complex (Dame et al. 1987)

Table 1. Surveyed ECC core catalogue (the first page of 22 pages)

Name	Glon (°)	Glat (°)	Ra(J2000) (h m s)	Dec(J2000) (d m s)	Ra(B1950) (h m s)	Dec(B1950) (d m s)	Region
G001.38+20.94	1.3842772	20.941952	16 34 38.06	-15 46 40.71	16 31 46.85	-15 40 30.16	Ophiuchus
G001.84+16.58	1.845703	16.587652	16 50 12.91	-18 04 22.37	16 47 18.48	-17 59 15.82	Ophiuchus
G003.73+16.39	3.7353513	16.393143	16 55 21.78	-16 43 35.31	16 52 28.86	-16 38 50.32	Ophiuchus
G003.73+18.30	3.7353513	18.308161	16 48 54.69	-15 36 02.09	16 46 03.29	-15 30 50.23	Ophiuchus
G004.02+16.64	4.0209961	16.646044	16 55 10.45	-16 21 23.27	16 52 17.98	-16 16 37.51	
G004.19+18.09	4.1967773	18.092196	16 50 42.47	-15 22 25.13	16 47 51.29	-15 17 20.75	
G004.15+35.77	4.152832	35.777241	15 53 29.82	-04 38 52.39	15 50 51.56	-04 30 01.93	High Glat
G004.17+36.67	4.1748047	36.678967	15 50 42.66	-04 04 20.84	15 48 05.00	-03 55 20.10	High Glat
G004.41+15.90	4.4165034	15.907708	16 58 35.99	-16 28 36.07	16 55 43.28	-16 24 04.69	
G004.46+16.64	4.4604487	16.646044	16 56 11.73	-16 00 51.08	16 53 19.65	-15 56 09.62	
G004.54+36.74	4.5483394	36.748764	15 51 14.27	-03 47 40.14	15 48 36.88	-03 38 41.35	High Glat
G004.81+37.02	4.8120112	37.028599	15 50 52.79	-03 27 20.38	15 48 15.74	-03 18 20.28	High Glat
G004.92+17.95	4.9218745	17.954901	16 52 50.41	-14 53 40.51	16 49 59.75	-14 48 45.05	
G005.03+19.07	5.0317378	19.076056	16 49 19.74	-14 09 20.80	16 46 30.04	-14 04 10.73	
G005.29+11.07	5.2954097	11.072874	17 17 19.97	-18 30 57.71	17 14 24.31	-18 27 45.91	
G005.29+14.47	5.2954097	14.477516	17 05 31.09	-16 36 07.96	17 02 38.08	-16 32 05.81	
G005.31+10.78	5.3173823	10.78794	17 18 23.02	-18 39 22.30	17 15 27.16	-18 36 15.00	
G005.69+36.84*	5.6909175	36.84193	15 53 11.88	-03 00 56.50	15 50 35.24	-02 52 04.98	High Glat
G005.80+19.92	5.8007808	19.926863	16 48 13.56	-13 04 14.26	16 45 25.16	-12 58 59.65	
G006.08+20.26	6.0864253	20.264484	16 47 44.35	-12 39 21.78	16 44 56.44	-12 34 05.17	
G006.04+36.74*	6.04248	36.748764	15 54 10.81	-02 50 56.32	15 51 34.33	-02 42 08.46	High Glat
G006.32+20.44	6.3281245	20.443523	16 47 40.85	-12 22 03.36	16 44 53.28	-12 16 46.52	
G006.41+20.56	6.4160151	20.562996	16 47 28.67	-12 13 52.53	16 44 41.26	-12 08 34.85	
G006.70+20.66	6.7016597	20.66263	16 47 46.71	-11 57 20.05	16 44 59.61	-11 52 03.63	
G006.96+00.89	6.965332	0.895288	17 57 59.28	-22 29 20.42	17 54 57.90	-22 29 05.02	4th Quad
G006.94+05.84	6.9433589	5.8479061	17 39 41.49	-19 58 05.07	17 36 43.62	-19 56 29.92	4th Quad
G006.98+20.72	6.9873042	20.722441	16 48 12.55	-11 42 10.17	16 45 25.73	-11 36 55.55	
G007.14+05.94	7.1411128	5.9416566	17 39 47.47	-19 45 05.14	17 36 49.87	-19 43 30.43	4th Quad
G007.53+21.10	7.5366206	21.101799	16 48 08.77	-11 03 53.56	16 45 22.69	-10 58 38.70	
G007.80+21.10	7.8002925	21.101799	16 48 43.20	-10 51 47.54	16 45 57.35	-10 46 35.08	

Results：

- All 674 clumps were observed, but 39 of the cores have reference position problem
- All were detected with 12CO and 13CO, 68% for C18O
- Double and three components were identified, 108 additional components were obtained for 12CO J=1-0

10% 13CO J=1-0 emission <3σ

50% C18O J=1-0 emission <3σ

:

Low mass

High mass

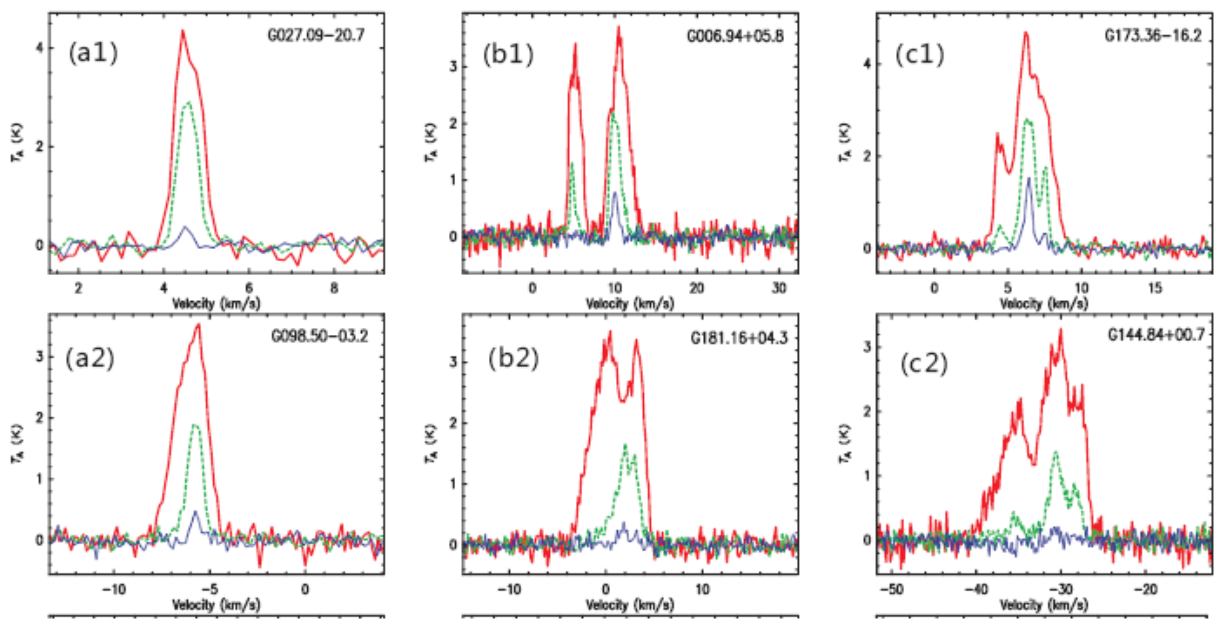

- Gaussian fitting： Vlsr, T, ΔV
- Characteristics of Line profiles

  Blue and red profiles (Zhou et al. 1993: Wu and Evans 2003)

  Red and blue wings, pedestal
- Theory of radiation transfer：

  Tex,

  tau, optical depth

  NH2, Column density
- Ten cores were mapped: 12 components, contours

Table 2. Observed parameters of the J=1-0 lines of ^{12}CO, ^{13}CO and $C^{18}O$ (the first page of 32 pages)

Name	$V_{lsr}(12)$ (km s^{-1})	FWHM(12) (km s^{-1})	$T_A(12)$ (K)	$V_{lsr}(13)$ (km s^{-1})	FWHM(13) (km s^{-1})	$T_A(13)$ (K)	$V_{lsr}(18)$ (km s^{-1})	FWHM(18) (km s^{-1})	$T_A(18)$ (K)	
G001.38+20.94	6.61(0.01)	1.16(0.02)	5.67(0.18)	0.7(0.01)	0.78(0.01)	3.98(0.09)	0.74(0.01)	0.54(0.03)	1.26(0.09)	
G001.84+16.58	6.05(0.01)	1.32(0.03)	5.58(0.17)	5.87(0.01)	0.69(0.01)	4(0.09)	5.87(0.01)	0.38(0.02)	1.67(0.09)	
G003.73+16.39	6.44(0.01)	1.11(0.02)	5.56(0.17)	6.17(0.01)	0.71(0.01)	3.41(0.09)	6.17(0.02)	0.53(0.07)	0.77(0.09)	RA
G003.73+18.30	4.44(0.01)	1.36(0.02)	6.68(0.21)	4.37(0.01)	0.97(0.01)	4.34(0.08)	4.32(0.01)	0.43(0.02)	2.45(0.08)	
G004.02+16.64	5.92(0.01)	0.69(0.02)	5.5(0.18)	5.87(0)	0.49(0.01)	3.81(0.09)	5.86(0.02)	0.34(0.05)	0.71(0.08)	
G004.19+18.09	3.64(0.01)	1.63(0.02)	5.94(0.19)	3.5(0.01)	1.23(0.01)	4.12(0.09)	3.73(0.02)	0.44(0.05)	0.94(0.08)	Dob
G004.19+18.09	6.68(0.01)	0.88(0.02)	6.63(0.19)	6.69(0.01)	0.62(0.01)	3.16(0.09)				
G004.15+35.77	2.47(0.01)	1.92(0.03)	4.72(0.14)	2.61(0.01)	1.06(0.02)	3.17(0.09)				
G004.17+36.67	2.55(0.01)	0.93(0.02)	5.08(0.17)	2.47(0.01)	0.71(0.01)	3.27(0.08)				
G004.41+15.90	4.78(0.01)	0.57(0.01)	6.11(0.15)	4.73(0)	0.48(0.01)	3.69(0.09)				
G004.46+16.64	5.16(0.01)	1.66(0.02)	6.1(0.15)	5.34(0.01)	1.19(0.02)	3.67(0.09)	5.55(0.01)	0.43(0.03)	1.42(0.09)	BA
G004.54+36.74	2.46(0.01)	1.17(0.02)	4.5(0.17)	2.53(0.01)	0.76(0.02)	2.94(0.09)	2.54(0.04)	0.44(0.1)	0.44(0.09)	BA
G004.81+37.02	3.6(0.01)	1.51(0.02)	4.47(0.13)	3.71(0.01)	1.04(0.02)	2.91(0.09)	3.82(0.04)	0.66(0.09)	0.46(0.08)	
G004.92+17.95	3.54(0.02)	1.49(0.03)	3.77(0.18)	3.72(0.01)	0.63(0.03)	3.26(0.17)	3.71(0.01)	0.32(0.03)	0.98(0.08)	
G005.03+19.07	3.83(0.01)	1.25(0.02)	7.17(0.19)	3.77(0.01)	0.99(0.01)	3.86(0.09)	3.81(0.03)	0.65(0.07)	0.73(0.09)	
G005.29+11.07	4.37(0.01)	0.92(0.01)	7.55(0.18)	4.22(0)	0.63(0.01)	4.07(0.09)	4.14(0.01)	0.34(0.04)	1.16(0.09)	
G005.29+14.47	3.76(0.01)	0.4(0.01)	5.07(0.18)	3.74(0.01)	0.3(0.02)	1.21(0.09)				
G005.31+10.78	4.53(0.01)	1.24(0.02)	6.56(0.19)	4.38(0.01)	0.88(0.01)	4.1(0.1)				RA
G005.69+36.84	0.56(0.03)	1.39(0.06)	3.84(0.17)	0.6(0.03)	0.96(0.07)	0.81(0.09)				Dob
G005.69+36.84	2.25(0.04)	1.62(0.08)	3.4(0.17)	2.33(0.01)	0.9(0.02)	3.01(0.09)	2.27(0.01)	0.4(0.02)	1.46(0.09)	
G005.80+19.92	3.45(0.01)	1.41(0.02)	6.11(0.18)	3.06(0.01)	0.89(0.01)	3.87(0.09)	2.96(0.02)	0.47(0.05)	0.99(0.09)	
G006.08+20.26	4.03(0.01)	1.95(0.02)	5.23(0.16)	3.96(0.01)	0.91(0.01)	4.19(0.08)	3.97(0.01)	0.56(0.03)	1.16(0.08)	BA*
G006.04+36.74	2.34(0.02)	1.99(0.04)	3.61(0.17)	2.61(0.01)	0.94(0.02)	2.73(0.1)	2.53(0.01)	0.47(0.03)	1.47(0.09)	RA
G006.32+20.44	4.48(0.01)	1.6(0.02)	4.98(0.16)	4.32(0.01)	0.72(0.01)	4.25(0.09)	4.27(0.01)	0.38(0.02)	1.88(0.09)	
G006.41+20.56	4.54(0.01)	1.38(0.02)	5.9(0.16)	4.39(0.01)	0.95(0.01)	4.43(0.08)	4.44(0.02)	0.67(0.04)	1.37(0.09)	
G006.70+20.66	3.49(0.01)	2(0.03)	4.44(0.15)	3.76(0.01)	1.06(0.01)	3.97(0.08)	3.79(0.01)	0.66(0.04)	1.35(0.09)	BA*

Table 3. Derived parameters of Surveyed ECC cores (The first page of 40 pages)

Name	V_{lsr} (km s^{-1})	R (kpc)	D (kpc)	Z (kpc)	T_{ex} (K)	τ(13)	N(13) (10^{16} cm^{-2})	τ(18)	N(18) (10^{15} cm^{-2})	N_{H_2} (10^{21} cm^{-2})	ratio(12/13)	X13/X18 (km s^{-1})	σ_{NT} (km s^{-1})	σ_{Therm} (km s^{-1})	σ_{3D}
G001.38+20.94	0.74	7.47	1.1	0.39	14.8	1.2	7.3	0.2	1.6	6.5	2.1	4.6	0.32	0.21	0.67
G001.84+16.58	5.87	4.51	4.16	1.19	14.6	1.2	6.5	0.4	1.5	5.7	2.7	4.3	0.29	0.21	0.61
G003.73+16.39	6.17	5.87	2.75	0.78	14.6	0.9	5.7	0.1	1.0	5.0	2.5	5.9	0.29	0.21	0.63
G003.73+18.30	4.32	6.48	2.14	0.67	16.8	1.0	10.6	0.5	2.7	9.4	2.2	4.0	0.41	0.23	0.80
G004.02+16.64	5.86	6.10	2.52	0.72	14.4	1.2	4.3	0.1	0.6	3.9	2.0	7.7	0.20	0.21	0.50
G004.19+18.09	3.73	6.88	1.71	0.53	15.3	1.2	12.1	0.2	1.0	10.8	1.9	12.2	0.52	0.22	0.97
G004.19+18.09	6.69	5.92	2.73	0.85	16.7	0.6	4.9			4.4	3.0		0.25	0.23	0.59
G004.15+35.77	2.61	7.13	1.7	0.99	12.9	1.1	7.4			6.6	2.7		0.45	0.20	0.85
G004.17+36.67	2.47	7.19	1.64	0.98	13.6	1.0	5.2			4.7	2.0		0.29	0.20	0.62
G004.41+15.90	4.73	6.62	1.96	0.54	15.7	0.9	4.3			3.8	2.0		0.19	0.22	0.50
G004.46+16.64	5.55	6.37	2.23	0.64	15.6	0.9	10.6	0.3	1.5	9.4	2.3	7.1	0.50	0.22	0.95
G004.54+36.74	2.54	7.25	1.56	0.93	12.4	1.0	4.9	0.1	0.4	4.3	2.4	11.5	0.32	0.19	0.64
G004.81+37.02	3.82	6.79	2.15	1.30	12.3	1.0	6.6	0.1	0.7	5.9	2.2	9.9	0.44	0.19	0.83
G004.92+17.95	3.71	7.10	1.48	0.46	10.9	2.0	4.3	0.3	0.7	3.8	2.7	6.5	0.26	0.18	0.55
G005.03+19.07	3.81	7.08	1.5	0.49	17.8	0.8	9.9	0.1	1.2	8.8	2.3	8.0	0.41	0.23	0.82
G005.29+11.07	4.14	7.09	1.44	0.28	18.6	0.8	6.8	0.2	1.1	6.1	2.7	6.5	0.26	0.24	0.61
G005.29+14.47	3.74	7.20	1.35	0.34	13.6	0.3	0.8			0.7	5.6		0.11	0.20	0.40
G005.31+10.78	4.38	7.03	1.51	0.28	16.6	1.0	9.0			8.0	2.3		0.37	0.22	0.75
G005.69+36.84	0.6	8.33	0.21	0.13	11.1	0.2	1.6			1.4	6.9		0.40	0.18	0.77
G005.69+36.84	2.27	7.60	1.13	0.68	10.2	2.1	5.5	0.6	1.2	4.9	2.0	4.6	0.38	0.18	0.72
G005.80+19.92	2.96	7.52	1.05	0.36	15.7	1.0	8.3	0.2	1.1	7.4	2.5	7.4	0.37	0.22	0.75
G006.08+20.26	3.97	7.26	1.33	0.46	13.9	1.6	8.7	0.2	1.5	7.7	2.7	5.9	0.38	0.21	0.75

Results：1. Line center velocity; distance

- Basic parameter
- Histogram

  Normal distribution

  V12-V13

  V13-V18

- Correlation:

  V12vs. V13

  V13 vs. V18

  100%

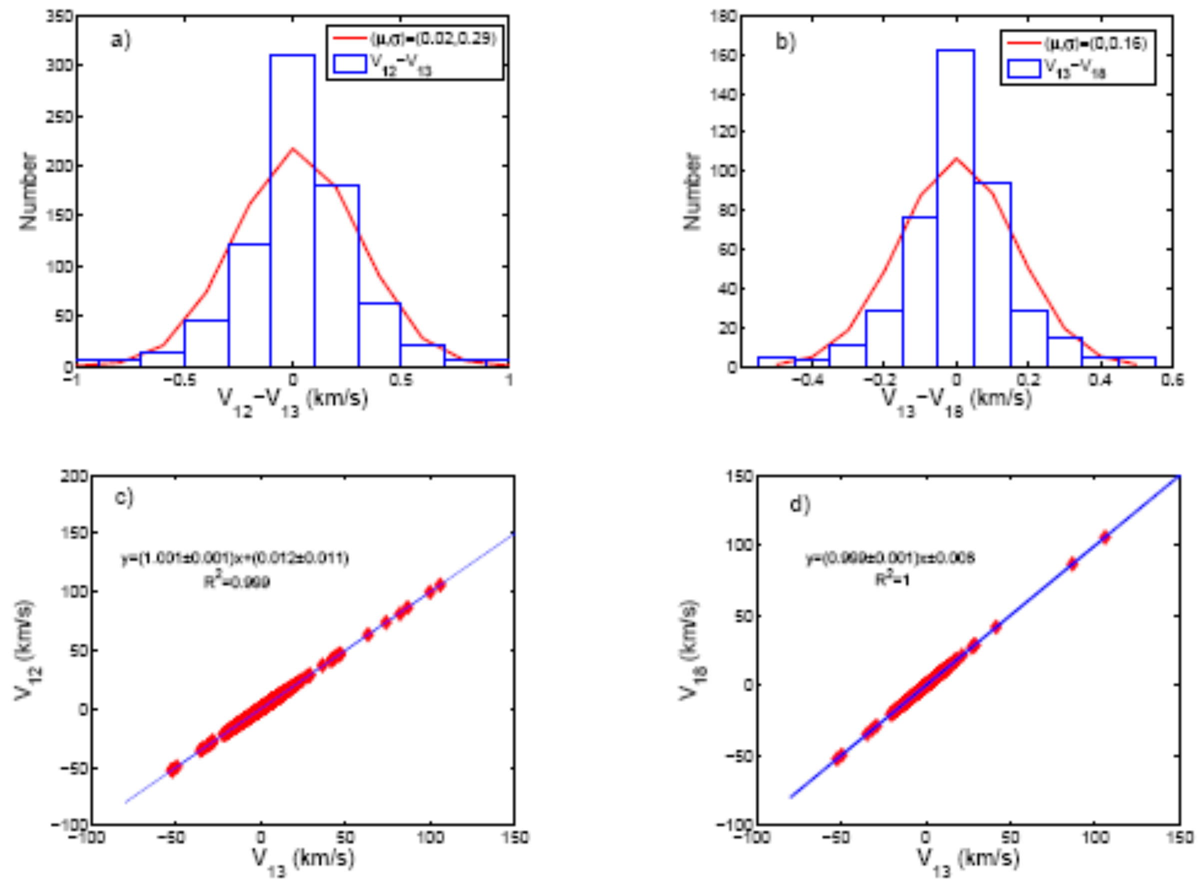

12CO, 13CO, C18O

Velocity difference between CO and its isotopes, any molecular lines is very common

In the 6 NH3 cores

Vlsr(12CO)-Vlsr(13CO)

(Zhang et al. 2011)

All are > 1 km/s

In SMA core of

G28.20-0.04

also > 1 km/s

(Qin et al. 2008)

Peak	Molecule	V_{LSR} (km s^{-1})	T_R^* (K)	ΔV (km s^{-1})	$\int T_R^* dV$ (K km s^{-1})	σ (K)
1	^{12}CO (1–0)	2.31	10.76	6.38	80.21±0.44	0.20
	^{13}CO (1–0)	0.96	5.00	3.19	31.44±0.22	0.22
	C^{18}O (1–0)	0.83	3.04	2.17	6.41±0.10	0.17
	HCO$^+$ (1–0)	1.44	1.00	4.78	4.99±0.28	0.21
2	^{12}CO (1–0)	2.67	11.02	6.47	80.02±0.72	0.33
	^{13}CO (1–0)	1.03	7.48	3.08	30.84±0.22	0.22
	C^{18}O (1–0)	1.04	2.75	1.83	5.21±0.13	0.21
	HCO$^+$ (1–0)	1.41	1.61	3.11	5.83±0.20	0.17
3	^{12}CO (1–0)	2.21	9.86	7.24	95.16±0.81	0.23
	^{13}CO (1–0)	0.90	5.87	4.05	25.53±0.25	0.25
	C^{18}O (1–0)	1.08	2.81	1.72	4.49±0.15	0.24
	HCO$^+$ (1–0)	−0.82	1.08	2.11	2.44±0.24	0.20
4	^{12}CO (1–0)	2.64	9.79	6.69	85.55±0.44	0.20
	^{13}CO (1–0)	1.11	5.71	3.30	25.15±0.21	0.20
	C^{18}O (1–0)	1.04	2.83	1.62	4.80±0.10	0.15
5	^{12}CO (1–0)	2.80	9.76	6.34	77.12±0.43	0.20
	^{13}CO (1–0)	1.32	5.87	3.14	23.28±0.21	0.21
	C^{18}O (1–0)	1.24	2.47	1.80	3.99±0.11	0.17
6	^{12}CO (1–0)	2.47	10.89	5.55	77.47±0.45	0.20
	^{13}CO (1–0)	1.67	8.34	2.70	25.82±0.23	0.23
	C^{18}O (1–0)	1.57	2.62	2.08	5.15±0.10	0.16
	HCO$^+$ (1–0)	2.08	1.35	3.33	4.91±0.19	0.16

Core 28.20-0.04 SMA

Table 1. Molecular Line Parameters

Molecule	Transition	Frequency (MHz)	E_u (K)	I_P (Jy beam^{-1})	ΔV (km s^{-1})	V_{LSR} (km s^{-1})	Channel rms (Jy beam^{-1})
CO^a	2–1	230538.00	17	–0.2±0.07	9.9±3.0	79.9±1.3	0.07
	…	…	…	–0.3±0.07	10.3±4.5	94.1±1.6	…
	…	…	…	0.28±0.09	7.1±2.1	103.1±1.3	…
$^{13}CO^a$	2–1	220398.68	16	–0.29±0.05	4.8±0.8	77.1±0.4	0.05
	…	…	…	0.3±0.05	6.3±0.9	104.3±0.4	…
OCS	19–18	231060.98	111	1.1±0.06	3.7±0.2	95.4±0.1	0.06
SO_2	$11_{1,11}–10_{0,10}$	221965.21	60	1.5±0.07	4.1±0.2	95.7±0.1	0.07
CH_3OH A	$10_2–9_3$	231281.10	166	0.3±0.07	4.6±0.8	95.5±0.3	0.07
CH_3CN	$12_0–11_0{}^b$	220747.26	69	1.1±0.08	3.8±0.3	95.1±0.1	0.08
	$12_1–11_1{}^b$	220743.01	76	1.2±0.08	4.9±0.4	95.0±0.1	0.08
	$12_2–11_2$	220730.26	97	0.9±0.08	4.1±0.3	95.3±0.1	0.08
	$12_3–11_3$	220709.02	133	1.0±0.08	4.2±0.3	95.4±0.1	0.08
	$12_4–11_4$	220679.29	183	0.6±0.08	4.8±0.5	95.4±0.2	0.08
	$12_5–11_5$	220641.09	247	0.7±0.07	3.9±0.3	95.3±0.1	0.07
	$12_6–11_6$	220594.43	325	0.6±0.08	3.3±0.4	95.8±0.2	0.08
$H30\alpha^c$	…	231900.96	…	0.9±0.2	20.9±0.6	92.5±0.2	0.06

- The agreement was revealed for the first time
- Important for initial conditions of star formation

Center velocity of molecular lines –dynamic layer of the molecular regions

The relation of different lines can provide clue to find initial states of star formation

- System velocity: 13CO line more optical thin than 12CO,
  also more common than C18 O

→V13 center velocity- system velocity

- A concrete application→ kinematic distance of the cores

Planck team: found kinematic D for 127 cores from infrared dark clouds (Simon et al. 2006) , most are on Galactic plane

Vlsr—dynamic distance:

- 82% < 2 kpc
- 51%: 0.5 –1.5 kpc

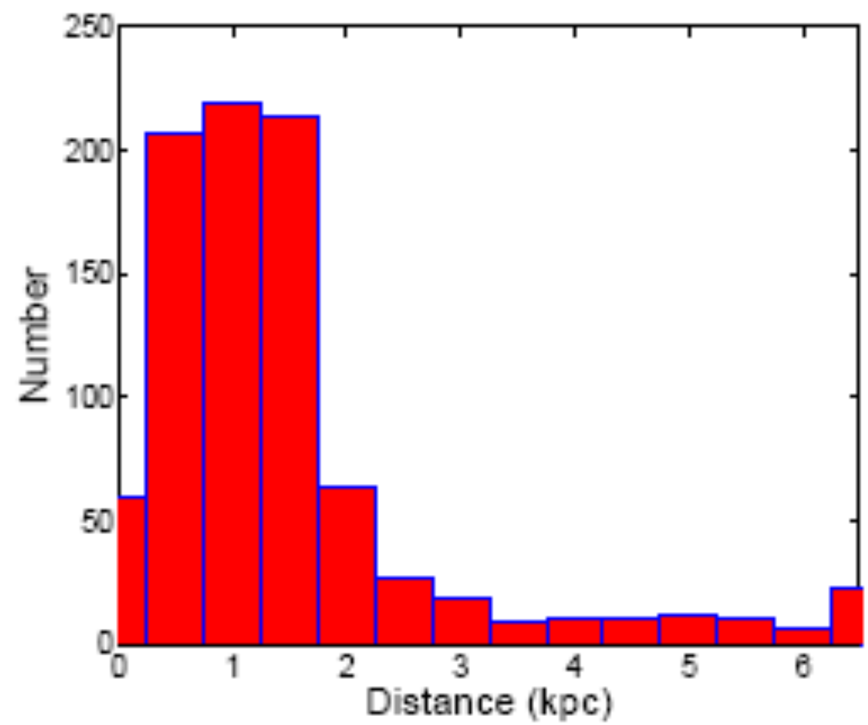

Results: 2. Physical parameters and line profile

Excitation temperature: Derived from T12

- Theory of radiation transfer
- Assuming T12 optical thick

$$T_{ex} = T_0/\ln[T_0(T_R^* + T_0e^{(-T_0/T_{bg})} - 1)]$$

- If the system is LTE, then kinematic temperature Tk obtained

  Range: 3.9 –27 K wider than that of Td: 7- 17 K

  Higher part:

  12 with Tk > 17 K,

  all are located in Orion and Tauri

  Lower part: additional components

  dust emission are not resolved yet

- Property of distribution:

  some deviated from lognomal distrit

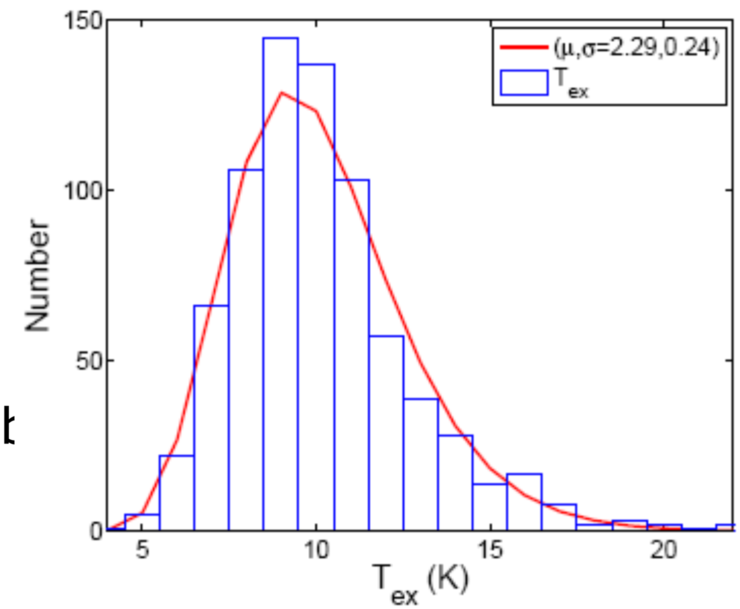

Line widths: Observed FWHM:

Most of the cores with narrow lines

- A criterion: 1.3 km/s for High-mass and Low-mass cores (Myers et al. 2083; Wu et al. 2003; Wang et al. 2009)

  H: 162; the remain belong to L.

- Thermal and non-thermal velocity dispersion:

$$\sigma_{NT} = [\sigma^2_{^{13}CO} - \frac{kT_{ex}}{m_{^{13}CO}}]^{\frac{1}{2}}$$

$$\sigma_{Therm} = [\frac{kT_{ex}}{m_H \mu}]^{\frac{1}{2}}$$

  as well as σ3D were investigated

- Property of the distribution:

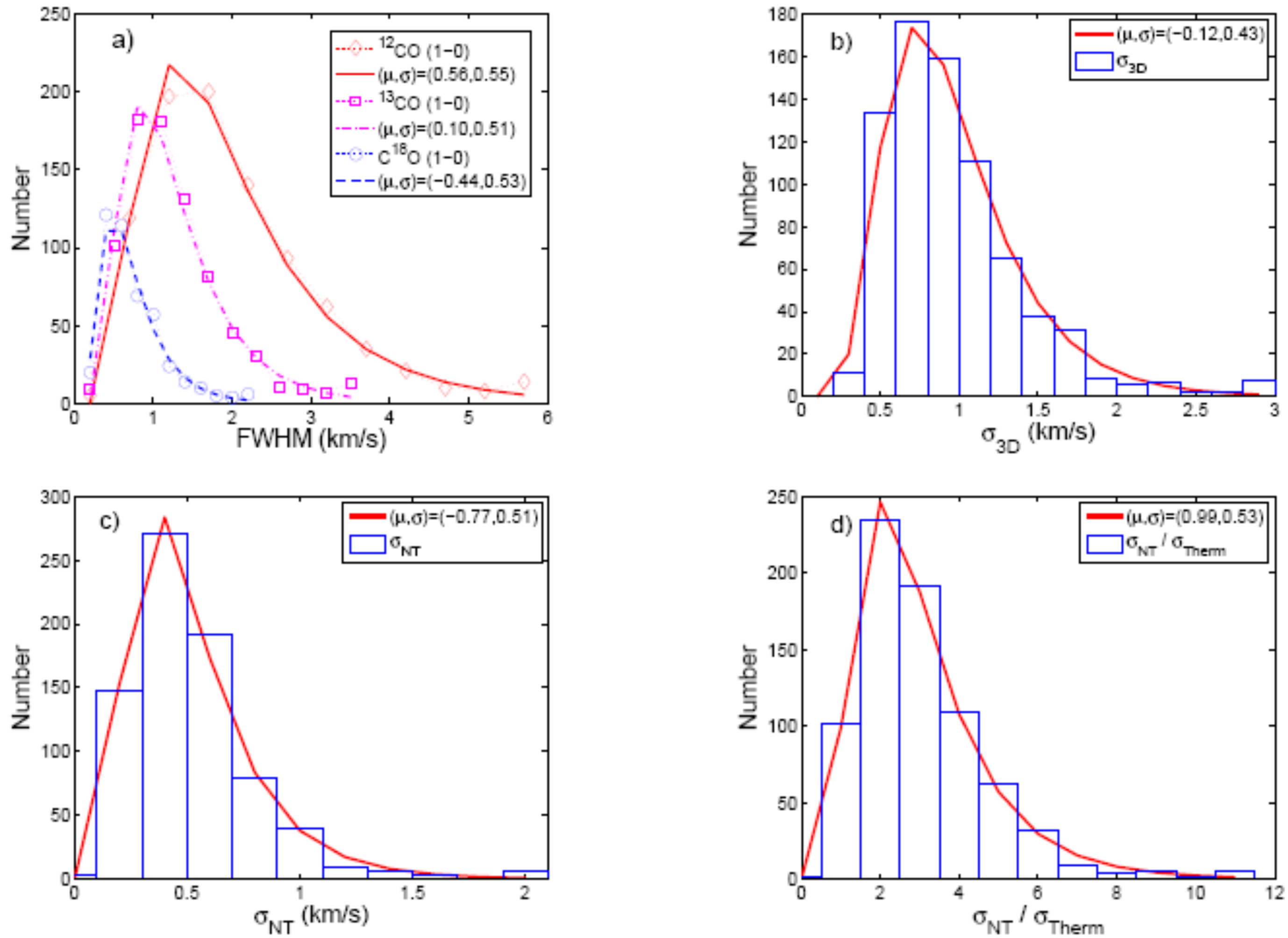

K-S test: All agree with lognomal distribution; σNT/ σThem some deviated

Column density NH2 :

- NH2 and the related optical depth tau13
  derived from tau13 with radiation transfer equation
  assuming 13CO line optical thin
- NH2 spans from 1020 to 4.5x1022 cm-3 , much larger than that of the nearby cores (Myers et al. 1983)
- Distribution:

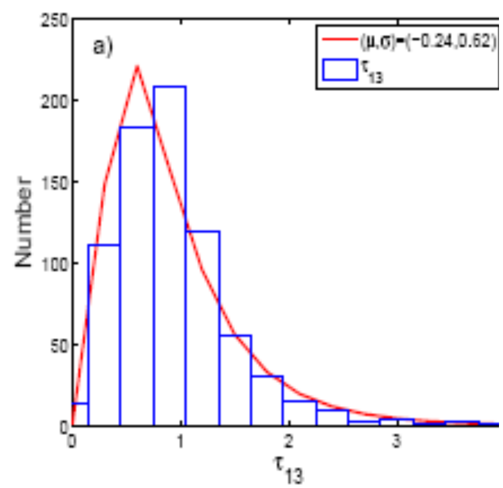

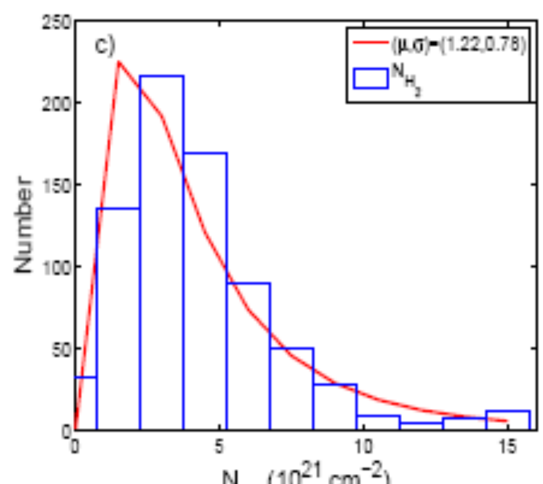

K-S test: Both are lognomal distribution + power larw tail

- Recently such distribution of NH2 was interpreted with part of the samples are in star formation (Froebrich et al. 2007; Goodman et al. 2009)
- The NH2 of the Planck cores with the same property,

  showing some of the cores are with star formation activities

But why?

- We have further obtained:

  Velocity dispersions: σNT, σThem , σ3D : lognormal with some tails

  Tex : Lognormal

  These are the factors to determine the column density– theory of radiation transfer

  We can see for Planck cores, NH2 is more depending on velocity dispersions, indication effect of turbuleance

Results: 3. Line profiles:

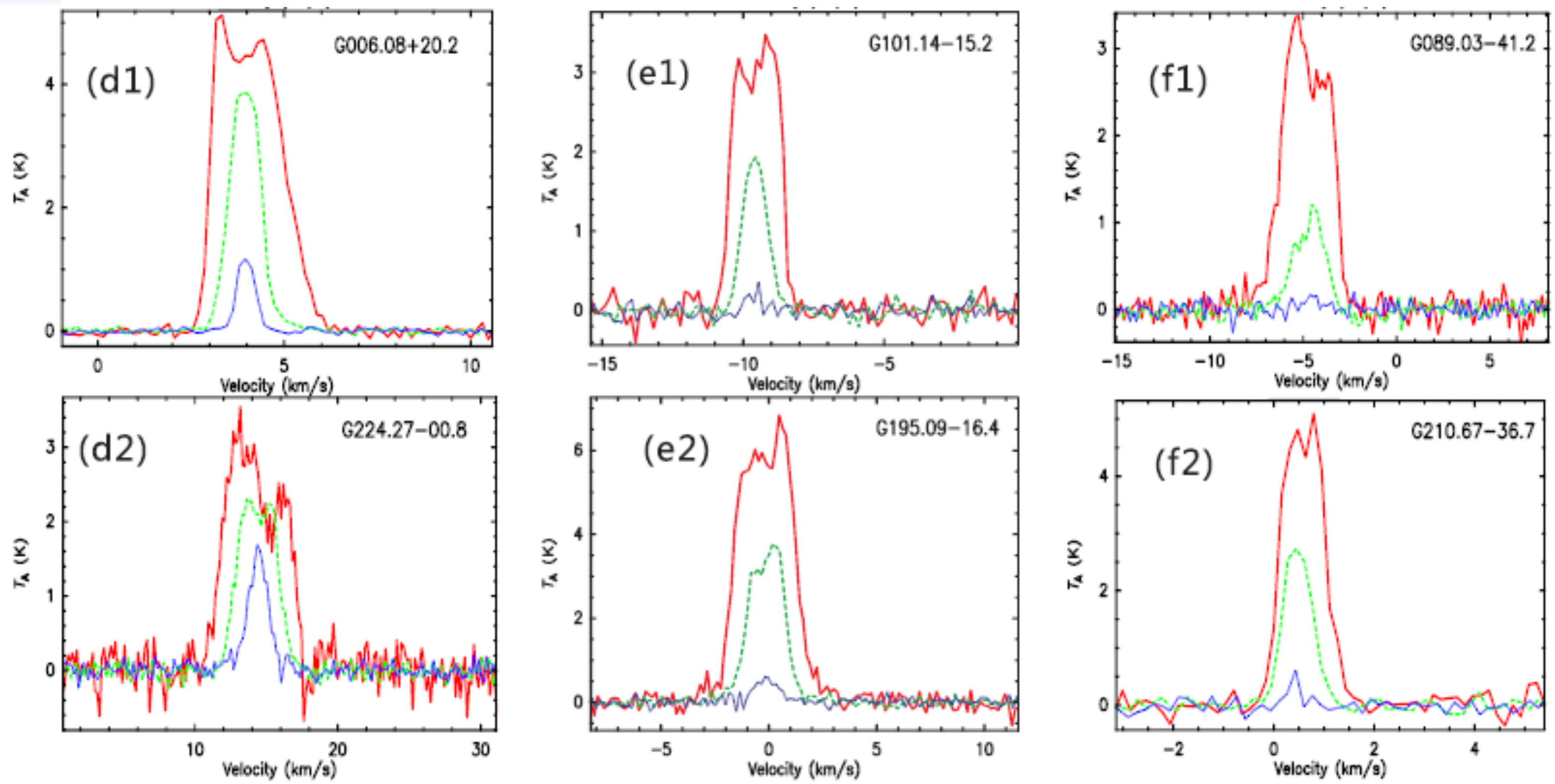

Blue Profile Red profile High Latitude

- 15 cores: center dip, absorption at the line center, rather symmetric
  8, dip shown in all the 3 lines– candidates of depletion
  7, dip only in 12CO , may be self absorption
- Blue asymmetric, 58 Red asymmetric ,40
- Blue profile, 15 (Nb) --2% Red profile, 5 (Nr) -- 0.8%
  small
- blue excess: E= (Nb-Nr)/Nt =0.01 (Nt=782) very small
  IRAM observation of HMPs and UCHII: 0.17 and 0.58 respectively (Wu et al. 2007)
- But blue profiles > red profiles, implying more cores are going to collapse than the protostellar objects driving mass outward

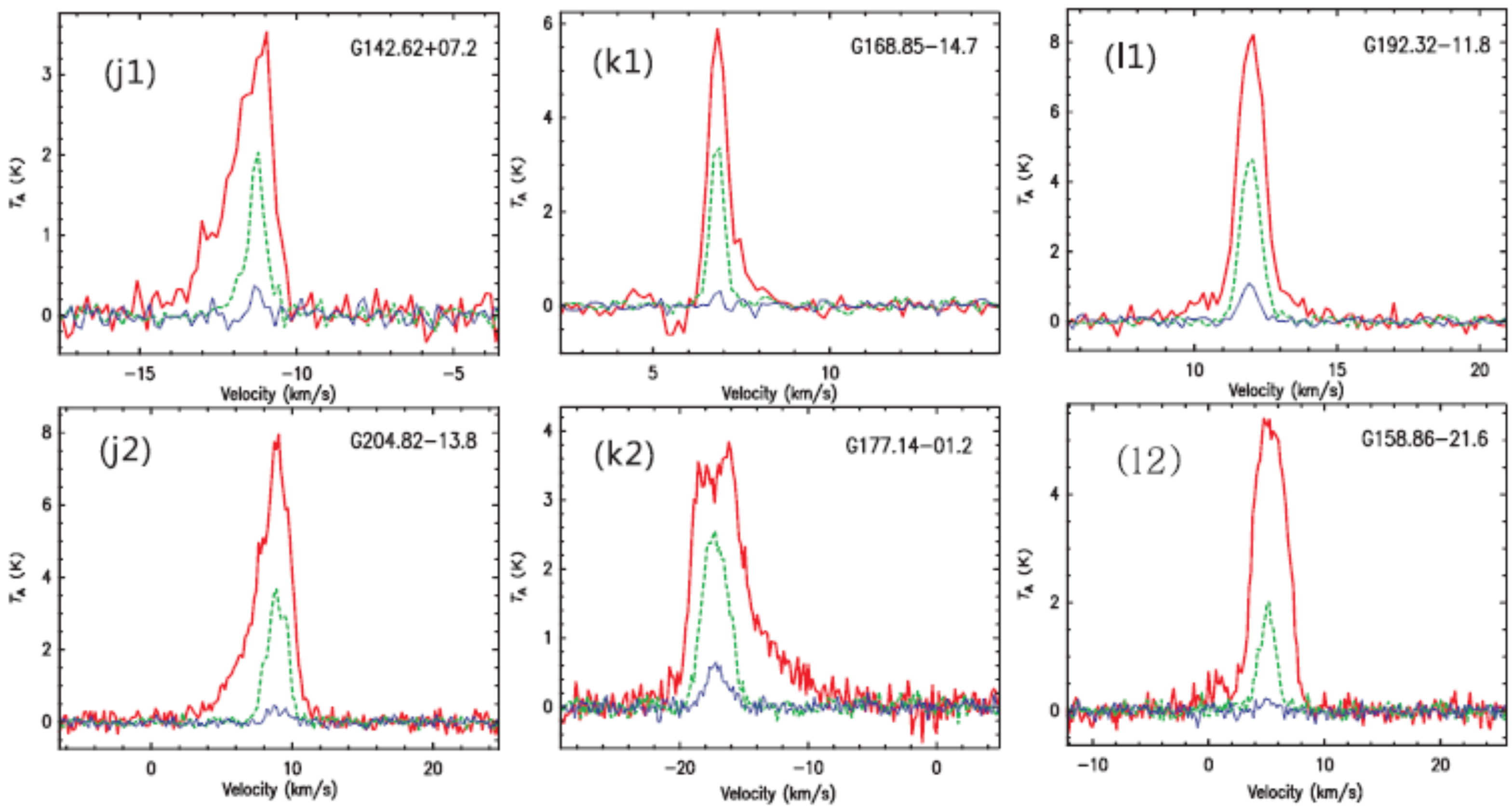

3 blue wing, 6 red, 8 both wings 5 pedestal

→ SF feed back or other HG are rare

Results: 4. Spatial distribution of the parameters

Tex:

With R:Tex > 10 K, R: 4—8 kpc
consistent with early
observations
(Scovile & Sanders 1987)

With Z.: high at 350, 450 pc

Velocity dispersions:

With R: Highest at 5 kpc
dynamic process is most
violent at 5 kpc ring

With Z: decrease from the disk
High again at ~680 pc minc
related with Orion, Tauri

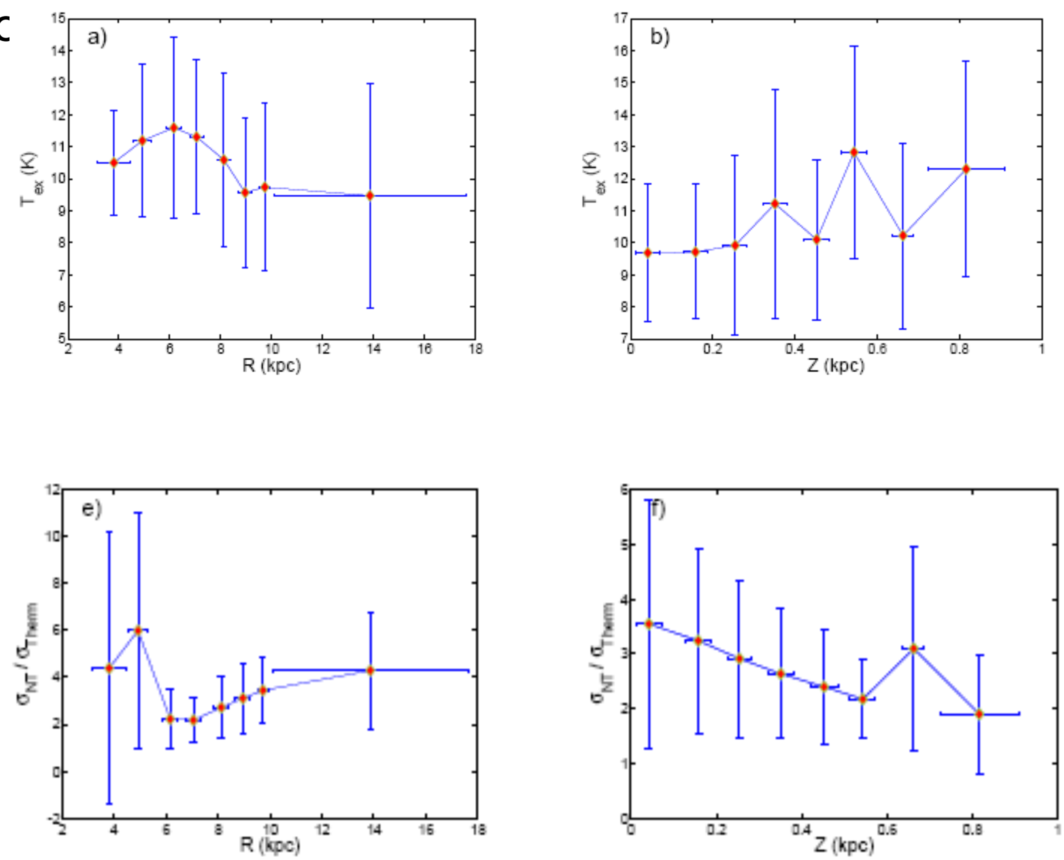

NH2(CO), NH2(flux 857μm):

With R:

Both increasing till 5 kpc, then decreasing till ~6 kpc

With Z:

NH2,a low valley at 450 pc

pflux 857μm: tending to be consistent

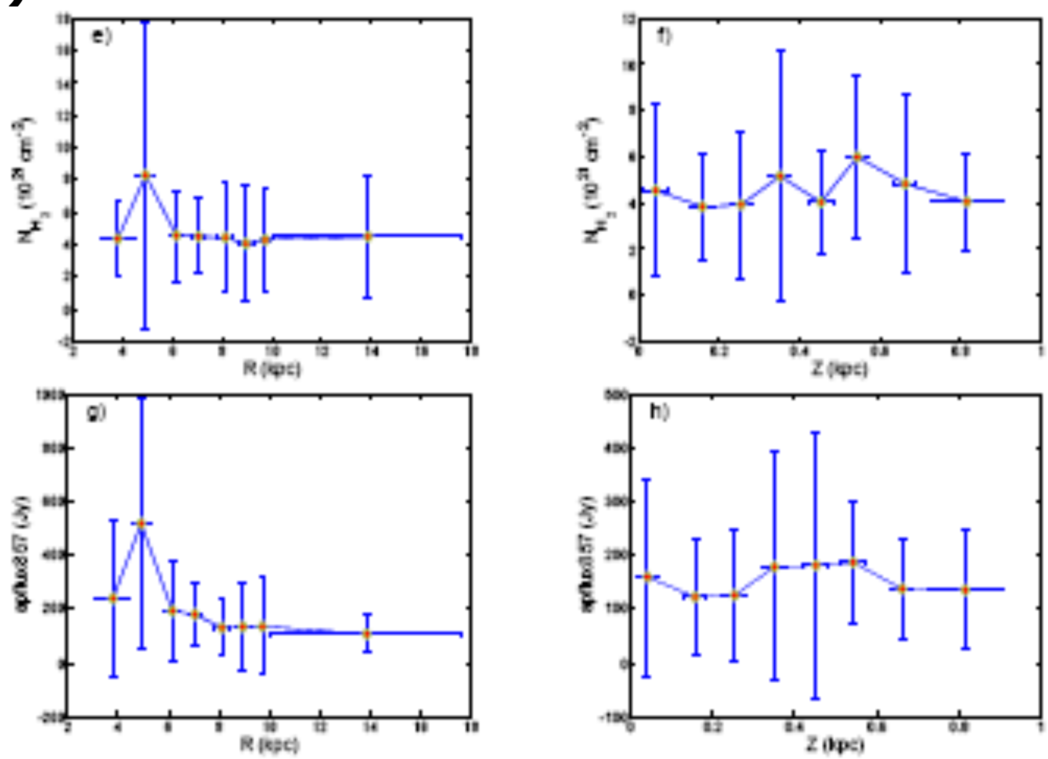

Parameters of different regions:

Table 5. Parameters of cores in different regions

region	l [°,°]	b [°,°]	Number	T_{12} (K)	T_{13} (K)	T_{18} (K)	FWHM(12) (km s^{-1})	FWHM(13) (km s^{-1})	FWHM(18) (km s^{-1})	N_{H2} (10^{21} cm^{-2})	T_{ex} (K)	τ(13)	X13/X18	σ_{NT} (km s^{-1})	σ_{Therm} (km s^{-1})	σ_{3D} (km s^{-1}
st Quad	[12,100]	[-10,10]	84	2.69(1.20)	1.85(0.77)	0.96(0.72)	2.70(2.23)	1.73(1.34)	0.96(0.72)	5.7(5.1)	9.4(2.4)	1.1(0.9)	5.6(3.3)	0.75(0.60)	0.17(0.02)	1.34(1.0
nd Quad	[98,180]	[-4,10]	70	2.57(1.23)	1.67(0.77)	0.85(0.51)	2.09(1.18)	1.42(0.68)	0.85(0.51)	4.5(3.4)	9.5(2.1)	0.9(0.5)	7.6(3.3)	0.62(0.29)	0.17(0.02)	1.13(0.4
th Quad	[180,279]	[-4,10]	43	2.57(1.11)	1.51(0.64)	1.05(0.40)	2.90(1.00)	1.74(0.67)	1.05(0.40)	4.7(2.6)	9.1(2.0)	0.7(0.3)	7.0(2.9)	0.73(0.28)	0.17(0.02)	1.31(0.4
Quad and Cir	[300,15]	[-8,8]	6	3.09(1.44)	1.54(0.59)	2.81(5.01)	3.03(2.57)	1.83(1.96)	2.81(5.01)	4.2(2.6)	9.5(0.9)	0.8(0.4)	4.4(2.3)	0.77(0.83)	0.17(0.01)	1.39(1.4
nticenter	[175,210]	[-9,7]	16	2.95(0.85)	1.90(0.77)	0.80(0.44)	2.63(1.09)	1.47(0.61)	0.80(0.44)	4.7(2.1)	9.3(1.7)	0.9(0.3)	7.6(1.1)	0.67(0.24)	0.17(0.02)	1.20(0.3
uila South	[27,40]	[-21,-10]	2	4.69(0.65)	2.78(0.63)	0.34(0.03)	0.83(0.16)	0.58(0.09)	0.34(0.03)	3.1(0.4)	12.8(1.3)	0.9(0.1)	9.0(0.2)	0.24(0.04)	0.20(0.01)	0.54(0.0
Cepheus	[99,143]	[8,22]	87	2.60(0.93)	1.66(0.64)	0.69(0.29)	1.94(0.87)	1.13(0.43)	0.69(0.29)	3.5(1.9)	8.8(1.8)	1.0(0.5)	5.4(2.1)	0.48(0.18)	0.16(0.02)	0.88(0.3
igh Glat		|b|≥25	41	3.30(1.12)	1.84(0.97)	0.46(0.18)	1.47(0.66)	0.89(0.40)	0.46(0.18)	3.0(2.0)	10.5(2.0)	0.8(0.5)	11.6(5.5)	0.37(0.17)	0.18(0.02)	0.72(0.2
Oph-Sgr	[8,40]	[9,24]	9	3.23(1.49)	2.11(1.08)	0.42(0.16)	1.30(0.46)	0.81(0.29)	0.42(0.16)	3.0(1.6)	10.2(2.7)	0.9(0.5)	6.1(2.9)	0.34(0.13)	0.18(0.02)	0.67(0.2
phiuchus	[344,4]	[7,25]	6	5.84(0.56)	3.89(0.40)	0.42(0.11)	1.10(0.23)	0.70(0.16)	0.42(0.11)	5.9(2.0)	15.0(1.2)	1.1(0.1)	7.0(5.6)	0.29(0.07)	0.21(0.01)	0.63(0.1
Orion	[180,225]	[-25,5]	82	3.58(1.90)	2.19(1.01)	0.76(0.35)	2.12(1.02)	1.29(0.53)	0.76(0.35)	5.8(5.3)	11.1(4.0)	1.0(0.6)	8.1(5.1)	0.55(0.23)	0.18(0.03)	1.02(0.3
Taurus	[152,180]	[-25,-3]	153	3.15(1.32)	2.08(0.86)	0.62(0.26)	1.67(0.78)	1.07(0.42)	0.62(0.26)	4.2(2.9)	10.3(2.6)	1.0(0.7)	6.2(3.4)	0.45(0.18)	0.18(0.02)	0.85(0.2
other			75	3.45(1.61)	1.97(1.22)	0.52(0.21)	1.51(0.68)	0.92(0.45)	0.52(0.21)	3.4(2.4)	10.5(3.3)	0.9(0.7)	7.4(4.4)	0.38(0.20)	0.18(0.03)	0.75(0.3

For cores at high latitude: 41 higher than 250

- the highest 710 , previous 440
- 5: belong to group H
- NH2: 3x1021 cm-2 , average, σNT smaller among the 12 regions regions but larger than that in Oph, Oph-Sgr, Tex: intermediate
- 3 BA: G004.54+36.74 Z: 930 pc
  G131.35-45.73 1200 pc
  G151.88-34.18 670 pc
- 3 RA: G006.64+36.74 2710 pc;
  G210.67-36.77 150 pc
  G161.43-35.59 was mapped
- Surveys: 16o≤b ≤ 44o 117o≤l ≤ 160o 13% CO detected(Heithausen ea 1993)

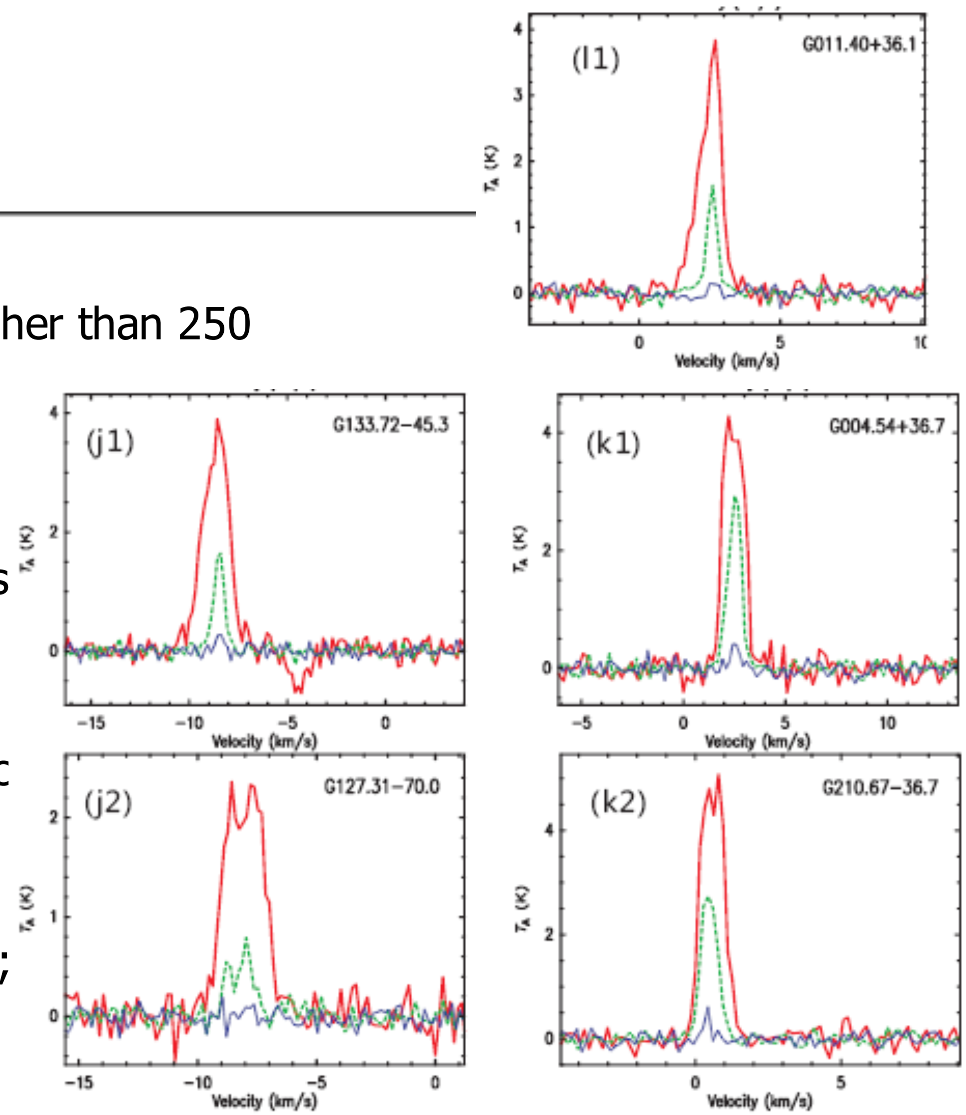

Results: 5. Mapping examples: 10 cores

Mapped 10 cores: 12 components, contours

- All the spectral parameters,
- Morphology, structure, associated objects were analyzed, 22 sub-cores
- Mapped parameters: sizes, density, mass MLTE, MJ, Mvir, derived

Status:

- 4 of the10 cores or 9 of the 22 sub-cores, filamentary or elongated shape
- In a state close to gravitational bound: 7: MLTE, > MJ and Mvir maybe under collapse; 7: agree within a factor of 3, likely gravitational stable
- Starless: 20 sub cores
- In a state that harbor infrared sources
- In a transition phase from diffuse ISM to cloud

For further study: molecular line, atomic line

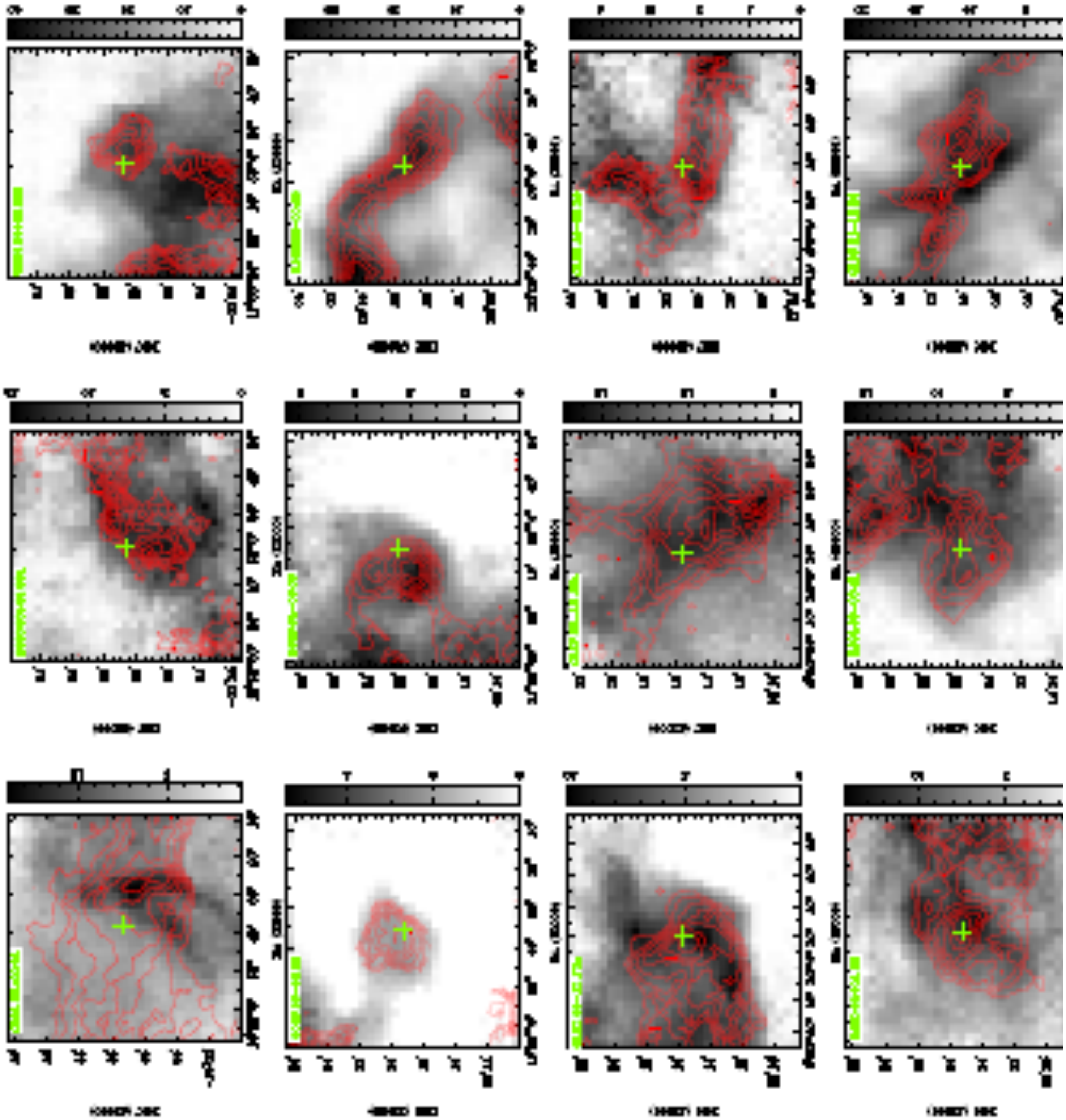

Table 6. Parameters of the ten mapped cores

Name	V_{lsr}	d	Offset	Deconvolved Size	R	T_{ex}	N_{H_2}	σ_{Therm}	σ_{NT}	σ_{3D}	n	M_{LTE}	M_{vir}	M_J	Morph	Group	Region
	km s^{-1}	(kpc)	($''$,$''$)	($'' \times ''$($^\circ$))	(pc)	(K)	(10^{21} cm^{-2})	(km s^{-1})	(km s^{-1})	(km s^{-1})	(10^3 cm^{-3})	($M_\odot$)	($M_\odot$)	($M_\odot$)			
G001.38+20.94	0.74	1.1	(-110,-41)	677×428(67.9)	1.4	14.1(0.9)	5.3(1.7)	0.21(0.01)	0.33(0.09)	0.67(0.13)	0.6	751	150	43	Diffuse	L	Ophiuchus
G006.96+00.89a	9.33	2.21	(5,-91)	187×119(-8.1)	0.8	9.9(0.4)	3.2(0.7)	0.17(0.00)	0.88(0.19)	1.56(0.32)	0.6	141	453	496	filament	H	4th Quad
	9.33	2.21	(-90,30)	149×102(-42.5)	0.7	9.7(0.5)	2.6(0.9)	0.17(0.00)	0.70(0.20)	1.25(0.34)	0.6	78	240	260	filament	H	4th Quad
	9.33	2.21	(-207,39)	301×64(-70.9)	0.7	9.4(0.3)	3.2(1.0)	0.17(0.00)	0.92(0.01)	1.61(0.17)	0.7	122	449	544	filament	H	4th Quad
	9.33	2.21	(-334,66)	268×143(89.1)	1.0	8.9(0.7)	2.7(0.7)	0.16(0.01)	1.02(0.30)	1.79(0.51)	0.4	204	783	945	filament	H	4th Quad
G006.96+00.89b	41.67	5.36	(-64,-1)	203×161(38.2)	2.3	10.7(1.1)	6.8(2.6)	0.18(0.01)	1.52(0.22)	2.66(0.37)	0.5	2579	3873	2905	core	H	4th Quad
G049.06-04.18	9.93	0.6	(16,41)	239×194(-51.9)	0.3	8.9(1.2)	1.3(0.5)	0.16(0.01)	0.15(0.04)	0.39(0.05)	0.7	9	11	7	Core	L	1st Quad
G089.64-06.59	12.51	0.6	(81,-20)	320×187(-0.9)	0.4	10.2(0.9)	3.4(1.5)	0.18(0.01)	0.40(0.09)	0.74(0.15)	1.5	30	45	38	Cometary	L	1st Quad
G108.85-00.80	-49.51	5.4	(-20,-12)	776×213(45.1)	5.3	11.5(3.7)	7.7(5.4)	0.18(0.03)	0.89(0.28)	1.58(0.46)	0.2	14993	3096	858	filament	H	2nd Quad
G157.60-12.17a	-7.75	1.17	(-38,-44)	432×283(16.4)	1.0	10.4(0.9)	3.6(1.2)	0.18(0.01)	0.40(0.01)	0.76(0.12)	0.6	243	133	61	Diffuse	L	Taurus
G157.60-12.17b	-2.58	0.47	(-83,-63)	535×421(41.7)	0.5	14.7(1.6)	4.1(1.5)	0.21(0.01)	0.43(0.11)	0.83(0.17)	1.2	82	87	55	Diffuse	L	Taurus
	-2.58	0.47	(-197,-278)	301×196(52.2)	0.3	14.6(1.3)	4.1(1.4)	0.21(0.01)	0.60(0.13)	1.11(0.21)	2.4	22	79	92	Diffuse	L	Taurus
G161.43-35.59	-5.83	1.49	(60,212)	269×143(-12.5)	0.7	9.8(0.4)	2.3(0.5)	0.17(0.00)	0.29(0.06)	0.59(0.08)	0.5	79	57	29	filament	L	High Glat
	-5.83	1.49	(-3,-40)	261×150(82)	0.7	12.0(1.2)	2.6(0.8)	0.19(0.01)	0.18(0.03)	0.46(0.04)	0.6	91	35	13	filament	L	High Glat
	-5.83	1.49	(-166,-71)	387×168(87.6)	0.9	10.5(0.9)	2.2(0.5)	0.18(0.01)	0.20(0.03)	0.47(0.04)	0.4	128	47	17	filament	L	High Glat
	-5.83	1.49	(-303,-86)	141×140(-21.1)	0.5	10.7(0.9)	1.9(0.6)	0.18(0.01)	0.25(0.06)	0.53(0.08)	0.6	34	33	21	filament	L	High Glat
G180.92+04.53	0.98	3.62	(0,-12)	359×339(62.2)	3.1	9.1(0.6)	3.4(1.1)	0.17(0.01)	0.59(0.11)	1.07(0.19)	0.2	2191	817	303	Diffuse	H	3th Quad
G194.80-03.41	12.84	2.89	(-4,-19)	690×341(81.3)	3.4	9.8(0.5)	4.5(1.7)	0.18(0.01)	0.86(0.31)	1.52(0.52)	0.2	3573	1829	812	dumbbell	H	3th Quad
	12.84	2.89	(-132,331)	355×242(61.3)	2.1	10.3(0.9)	5.3(2.4)	0.17(0.01)	0.78(0.20)	1.28(0.34)	0.4	1536	784	436	dumbbell	H	3th Quad
G196.21-15.50	3.76	0.8	(-79,5)	276×203(54.2)	0.5	14.5(0.8)	3.1(0.9)	0.21(0.01)	0.32(0.12)	0.68(0.16)	1.1	45	49	30	three cores	L	Orion
	3.76	0.8	(104,126)	228× 84(3.5)	0.3	15.1(0.8)	2.8(0.7)	0.21(0.01)	0.31(0.07)	0.65(0.11)	1.7	14	26	22	three cores	L	Orion
	3.76	0.8	(265,85)	256× 89(60.8)	0.3	14.6(0.6)	2.5(0.9)	0.21(0.00)	0.30(0.12)	0.66(0.15)	1.4	15	30	23	three cores	L	Orion

Results: 6. Evolutional states of the cores

Comparison of dust and gas:

- Td – Tk: Tk: the range > that of Td –SF
- NH2(CO) -- NH2(dust): NH2(CO) ranges 2.5 orders < NH2(dust)
- 1021-1021cm -2 critical value of cloud collapse (Hartquist & Williams 1998)

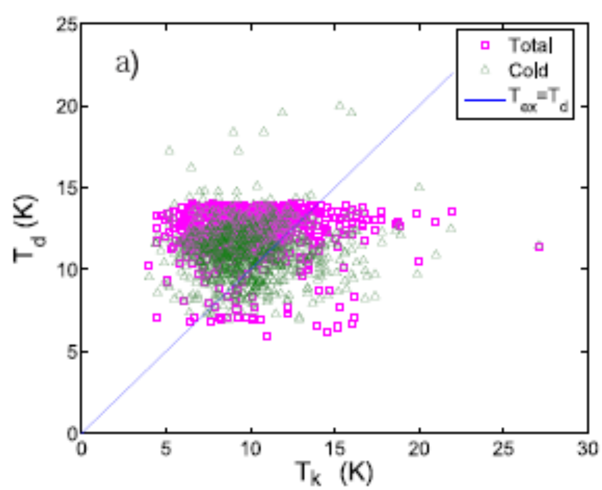

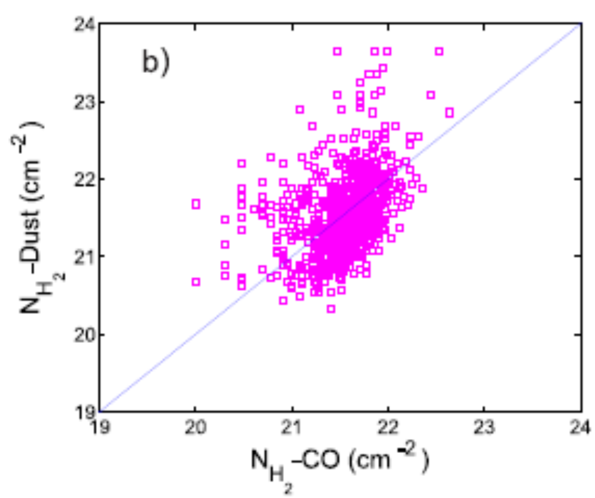

Comparison for cumulative of FWHM of 13CO lines and NH2 of different star formation samples

- FWHM: Methanol masers: largest
  Planck cores the smallest
- NH2: Column density: Planck cores the smallest too

Wu,Wu, Wang 2001
Shimon et al. 2006
Wang, Wu, Lan et al. 2009
Liu, Wu, Wang 2010
Chen, Shen, Xu et al. 20111

All are with with 13.7 m at Qinghai or FCRAO

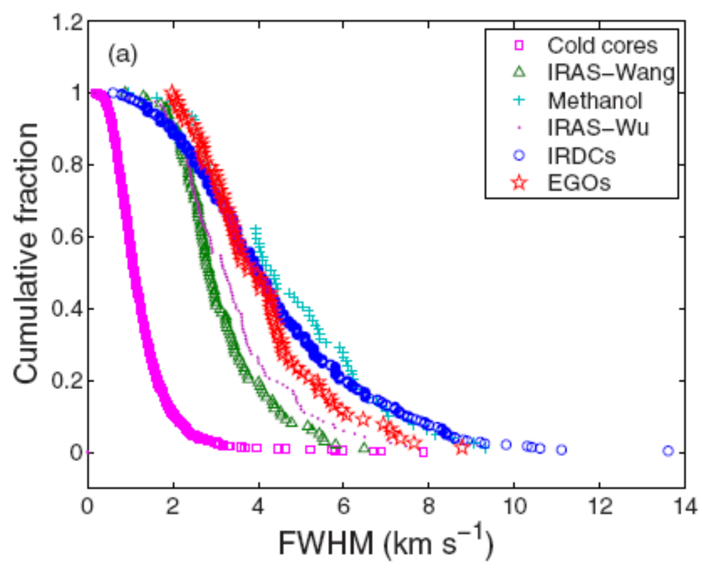

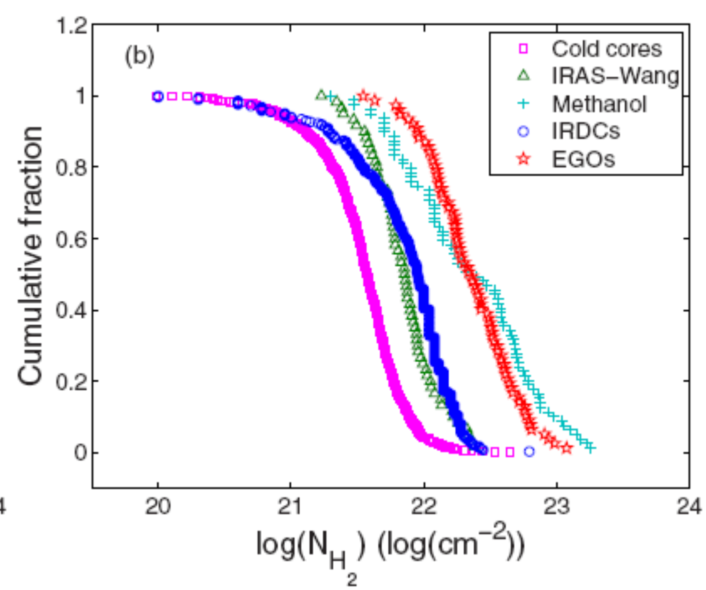

Orion Complex region: Liu, Wu Zhang, 2012

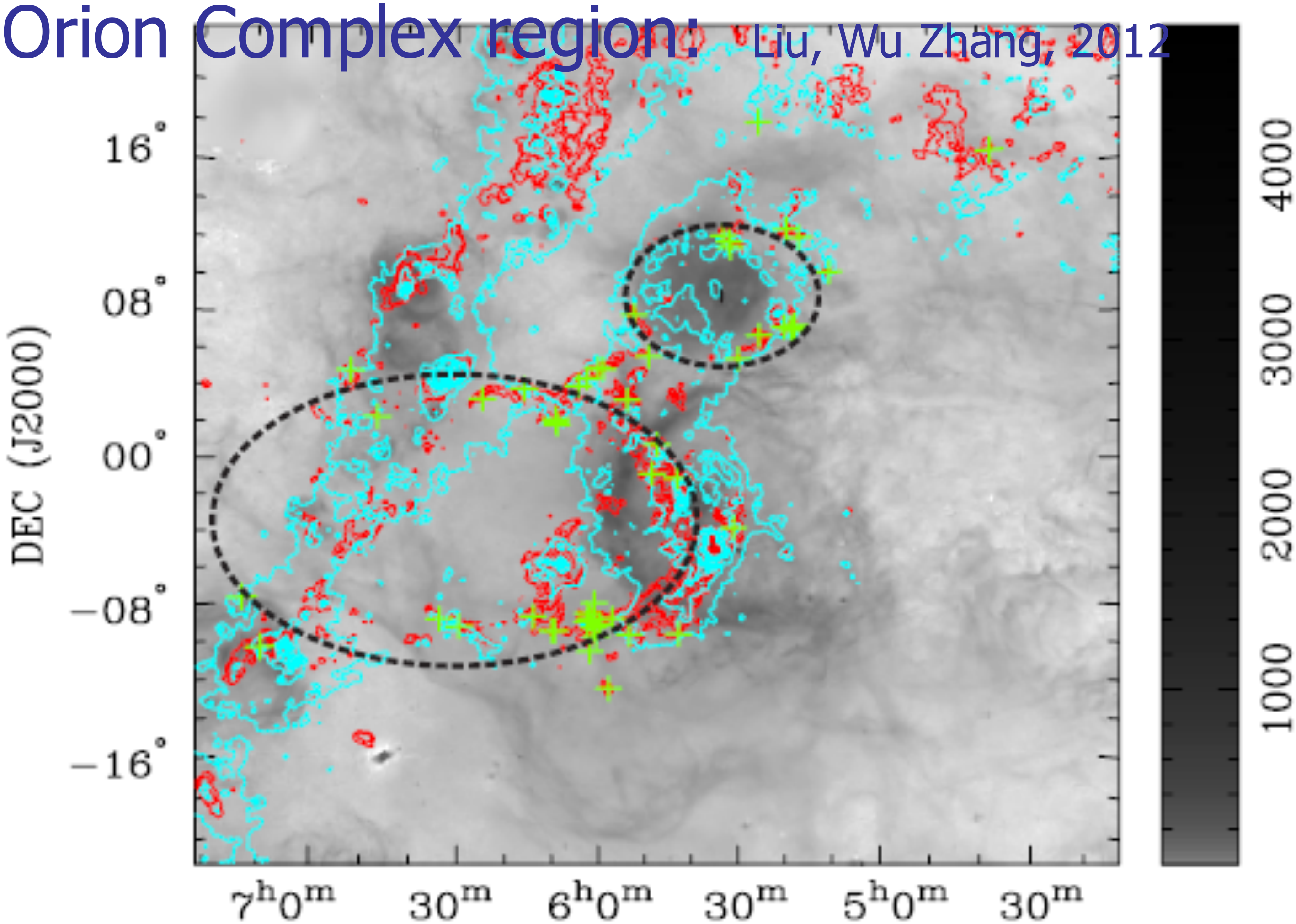

Back ground: Hα(Finkbeiner 03)
Green crosses :Planck clumps

Red contours: CO (Dame ea 01)
Blue contours: IRAS 100 μm

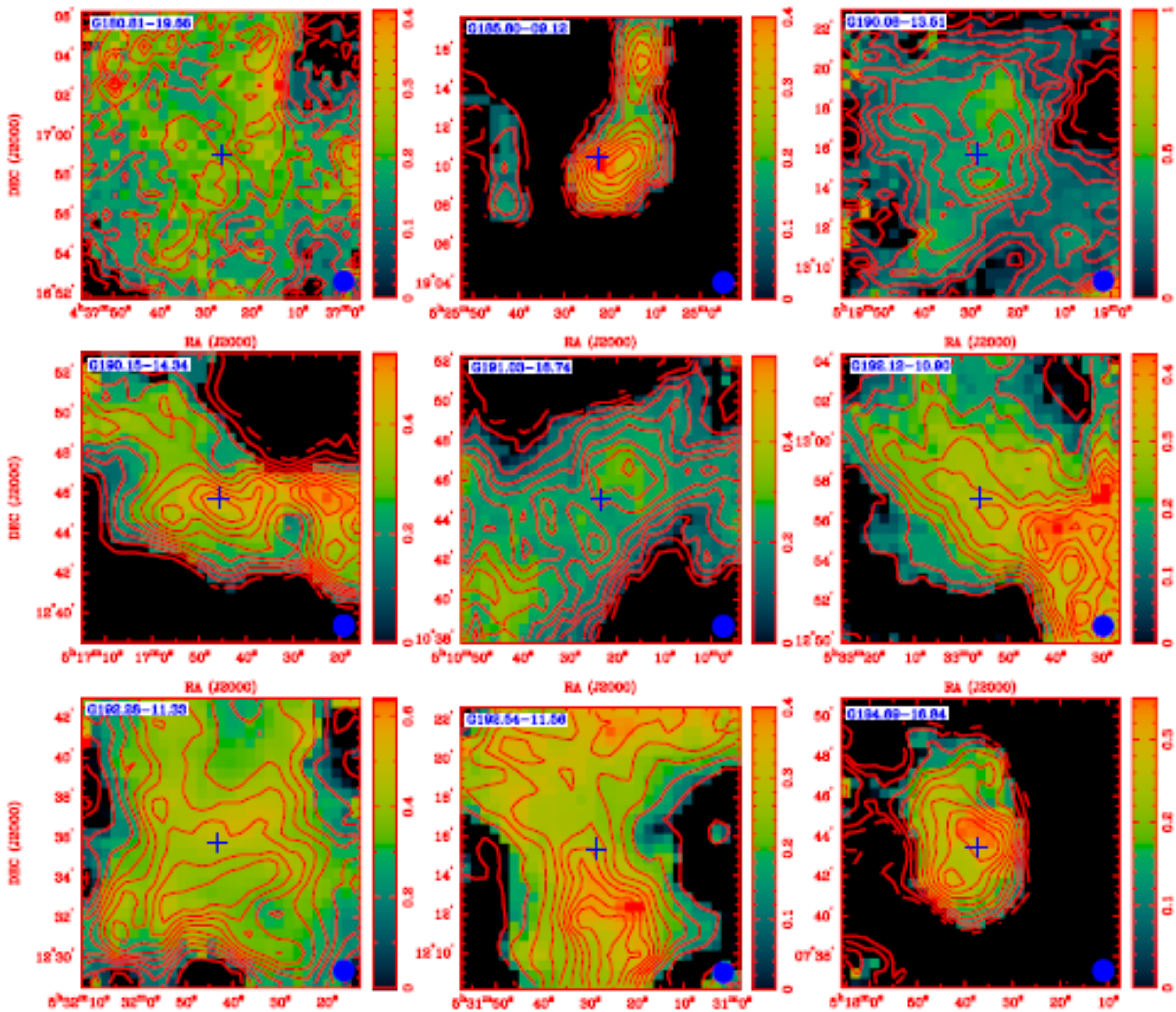

RA (J2000)
DEC (J2000)

Table 4. Derived parameters of the dense cores (First page of Table 4, the full table is only available on line)

Name	Deconvolved Size	R	V_{lsr}	n	M_{LTE}	M_{vir}	M_J	Remarks
	($'' \times ''$(°))	(pc)	(km s^{-1})	(10^3 cm^{-3})	($M_\odot$)	($M_\odot$)	($M_\odot$)	
G185.80-09.12	291×176(-42.8)	0.22	-2.8(0.1)	3.2	9.6	18.4	12.6	
	313×105(-7.6)	0.18	-2.3(0.1)	3.1	4.8	11.1	8.4	
G190.08-13.51	577×429(75.8)	0.54	1.2(0.2)	1.4	65.6	63.8	31.1	
	829×322(-25.5)	0.56	1.3(0.2)	1.4	70.8	73.9	38.3	
	153×121(-39.4)	0.15	1.3(0.1)	5.3	4.9	23.3	26.5	
	627×504(4.1)	0.61	1.4(0.3)	1.3	83.8	68.0	30.9	
G190.15-14.34	332×223(85.3)	0.30	1.5(0.2)	2.9	21.3	30.1	17.2	
	518×293(80.0)	0.42	1.4(0.1)	2.0	43.8	45.8	23.4	
	293×160(78.6)	0.24	1.5(0.2)	3.6	13.5	37.0	30.2	
G191.03-16.74	447×345(-65.9)	0.43	1.8(0.1)	1.4	31.0	28.0	13.3	
	440×397(33.6)	0.46	1.7(0.2)	1.3	35.2	29.8	13.7	
G192.12-10.90	948×337(51.4)	0.62	10.0(0.1)	1.9	127.7	57.0	19.0	
	302×265(85.9)	0.31	9.8(0.1)	3.8	32.0	35.2	18.4	
	339×192(7.5)	0.28	9.7(0.1)	4.5	27.7	33.6	18.8	
G192.28-11.33	336×255(-77.8)	0.32	10.1(0.2)	4.9	44.9	40.7	18.9	
	476×275(63.7)	0.39	10.4(0.1)	4.1	71.1	47.7	19.5	
	707×452(-70.7)	0.62	10.3(0.1)	2.6	175.0	94.3	34.7	
G192.54-11.56	605×302(11.3)	0.47	10.5(0.1)	3.9	112.2	53.2	18.4	

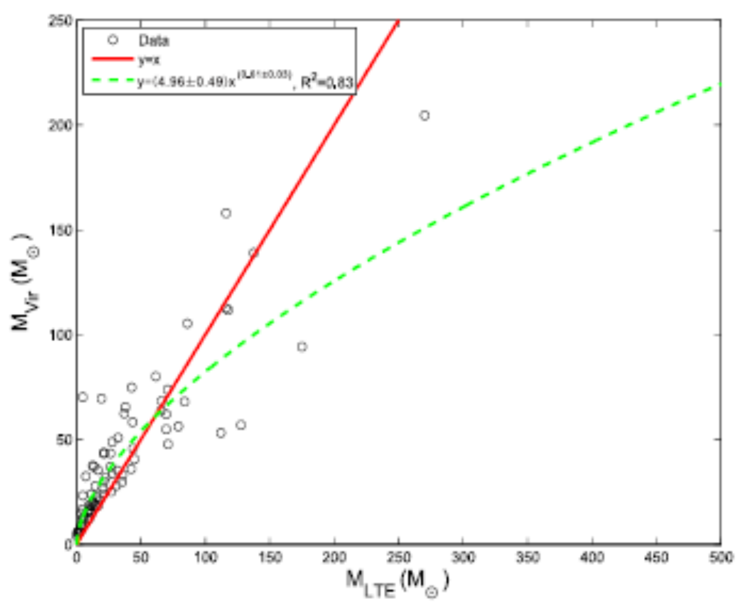

virias mass: LTE mass
~Orion B, Ikeda ea 09

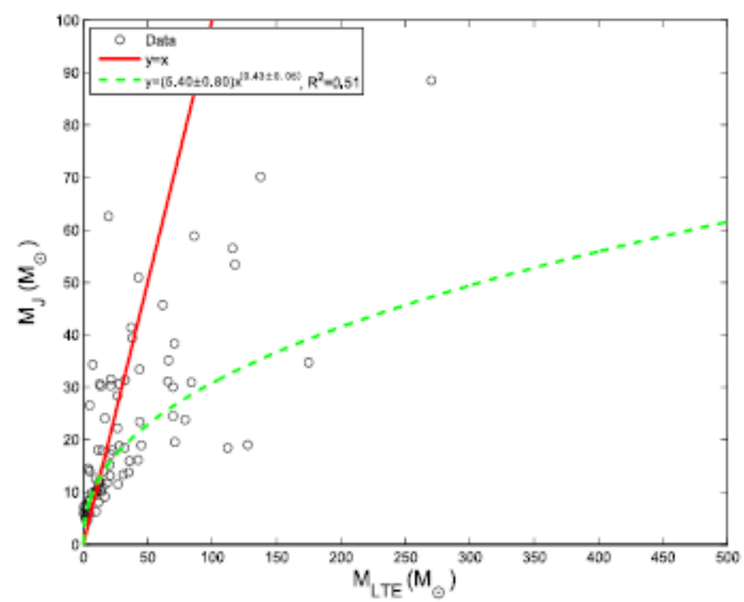

Jeans mass: LTE mass

=1.32±0.08. Compared with (2.35)

Core mass function: distribution:

$\alpha=1.32\pm0.08 < 2.35$

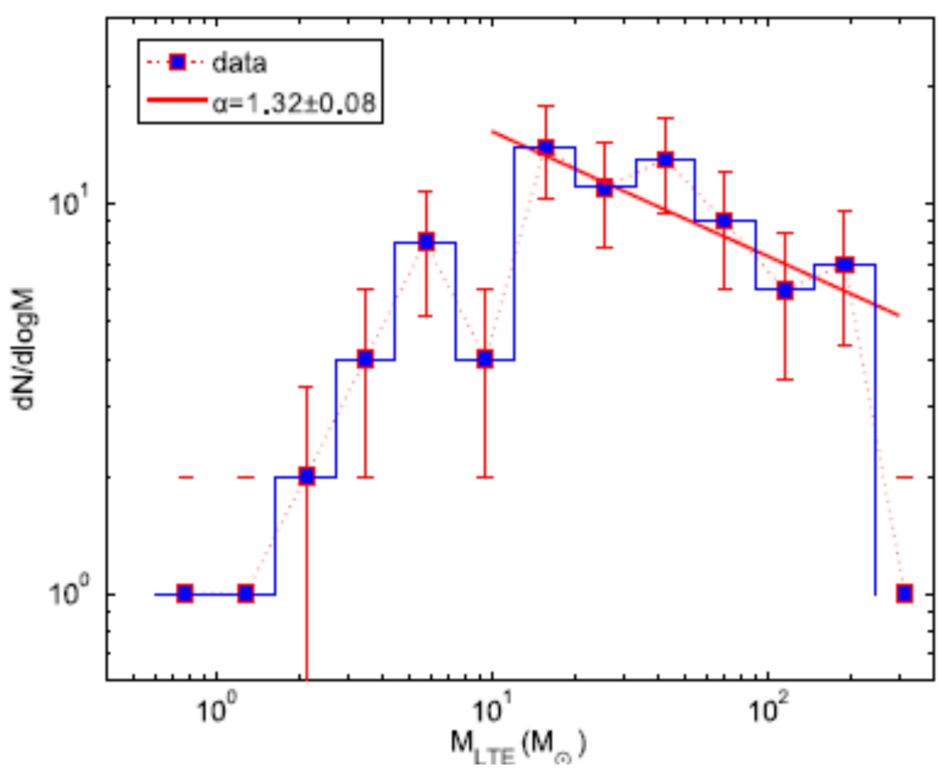

Mass cumulative

Red: The best lognormal distribution

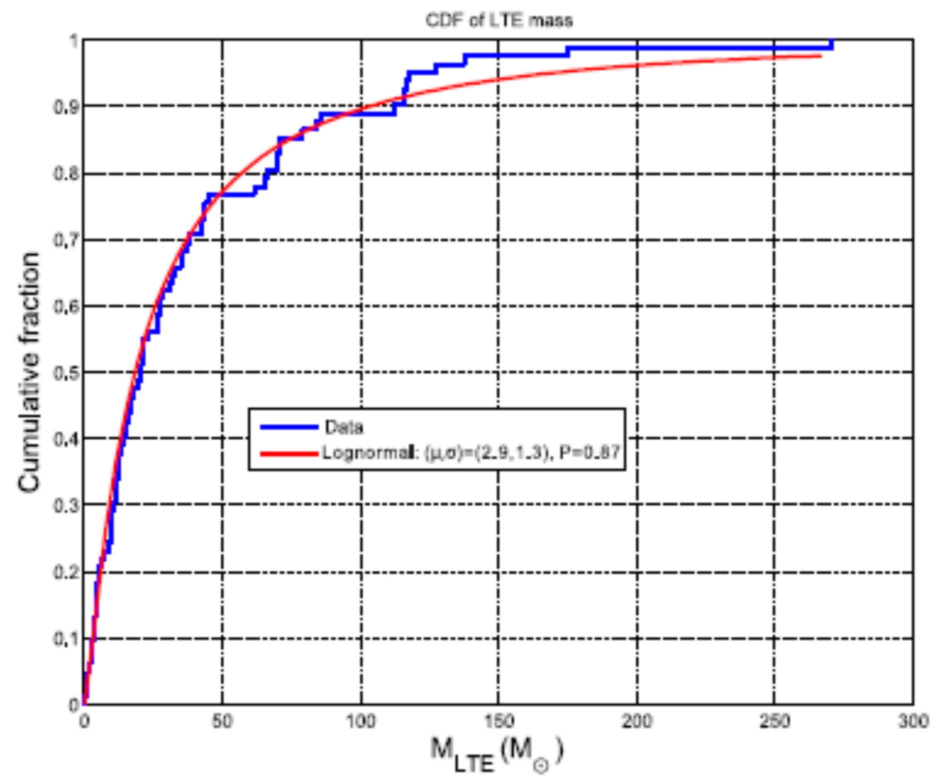

Taurus /Perseus/California regions:

Meng, Wu, Liu, 2013, ApJS, submitted

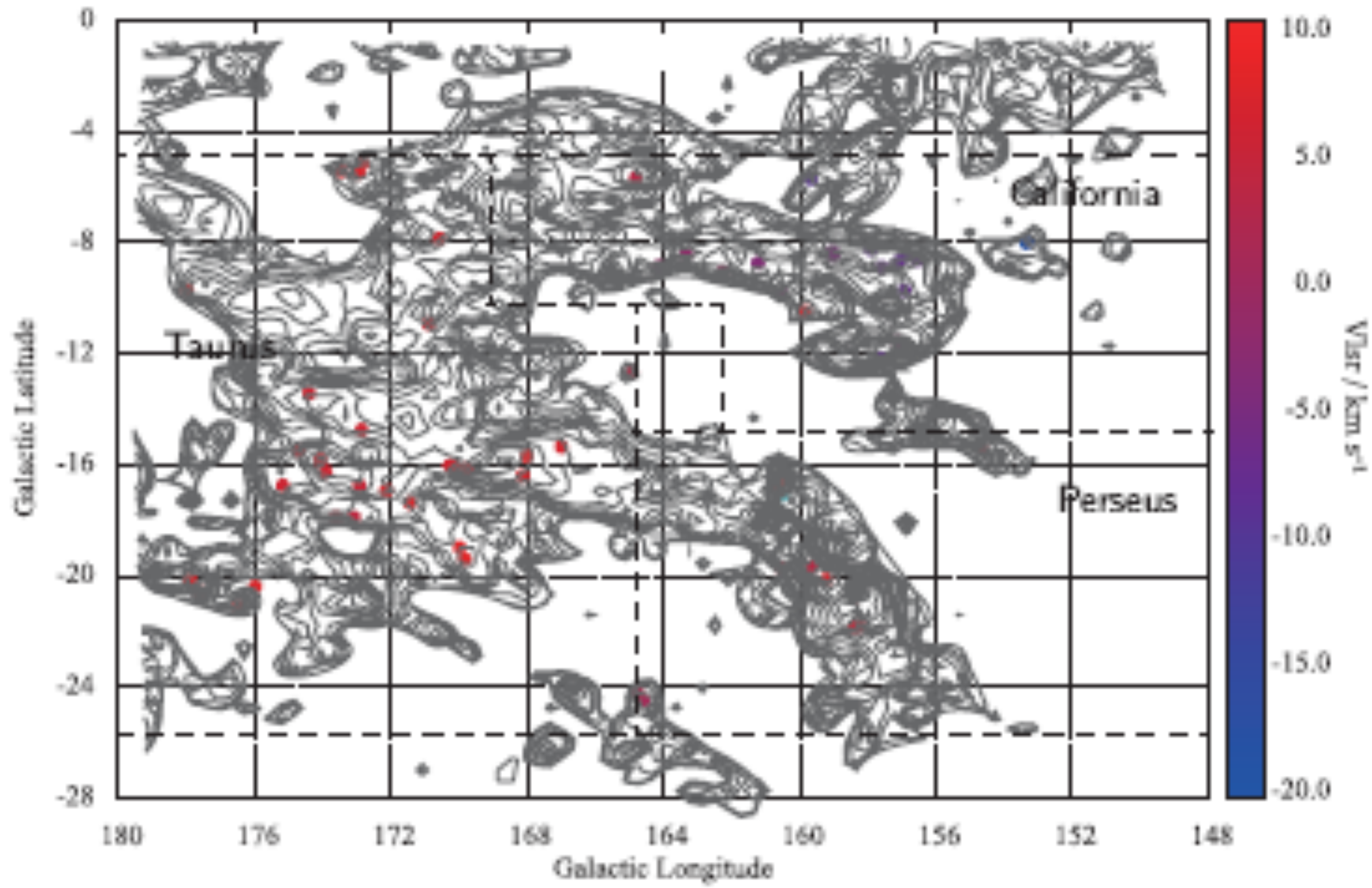

Contours: 13CO (Dame ea 01)
Colour dots: 13CO peak velocities

Dashed lines: 3 region boundaries (Lombardi ea 10)

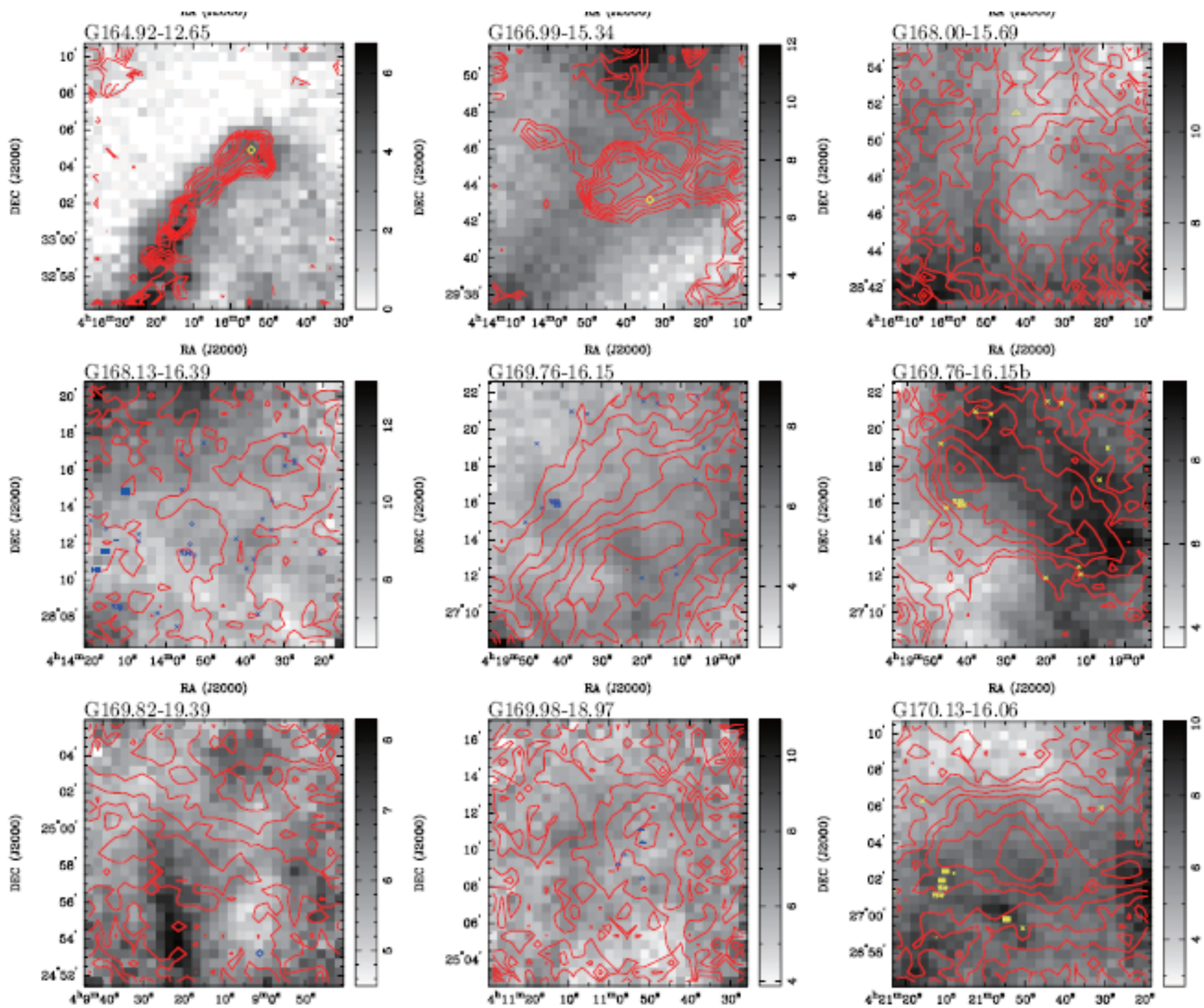
G164.92-12.65
G166.99-15.34
G168.00-15.69
G168.13-16.39
G169.76-16.15
G169.76-16.15b
G169.82-19.39
G169.98-18.97
G170.13-16.06
RA (J2000)
DEC (J2000)

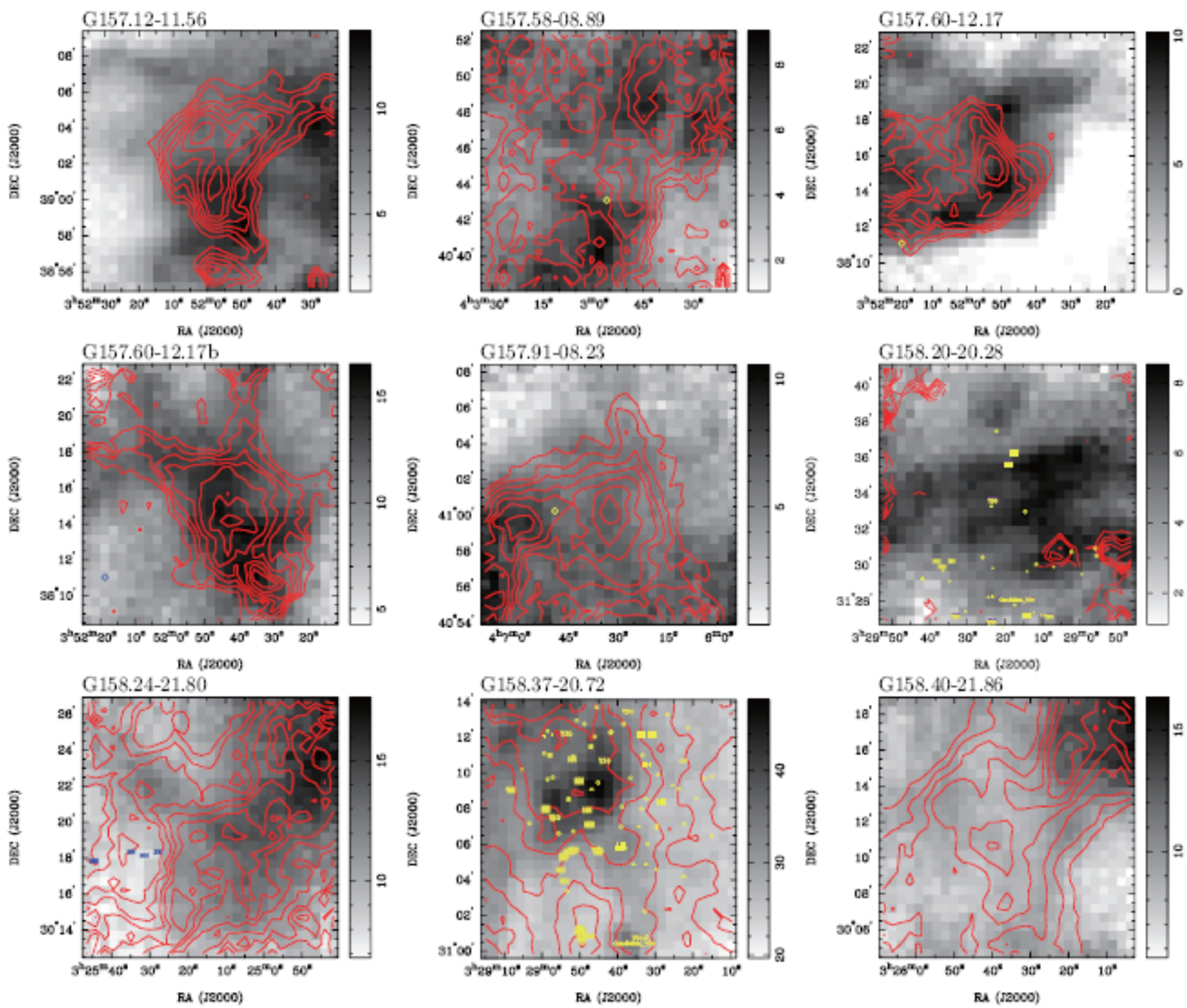
G157.12-11.56
G157.58-08.89
G157.60-12.17
G157.60-12.17b
G157.91-08.23
G158.20-20.28
G158.24-21.80
G158.37-20.72
G158.40-21.86
RA (J2000)
DEC (J2000)

Diffuse emission clumps seem to be more than those in Orion:

Two kinds:

Associated with YSOs

G158.37-20.72	TA: 12/13/18:	12/3.9/0.7
G174.06-15.81		4.89/3.88/1.36

Without YSO associated:

G169.78-16.15	TA: 12/13/18:	3.8/2.4/0.62
G169.98-18.97		3.9/2.5/0.61

Need statistics with significant samples

more larger maps

Evolution: ISM→molecular clouds→ISM

Four-steps:

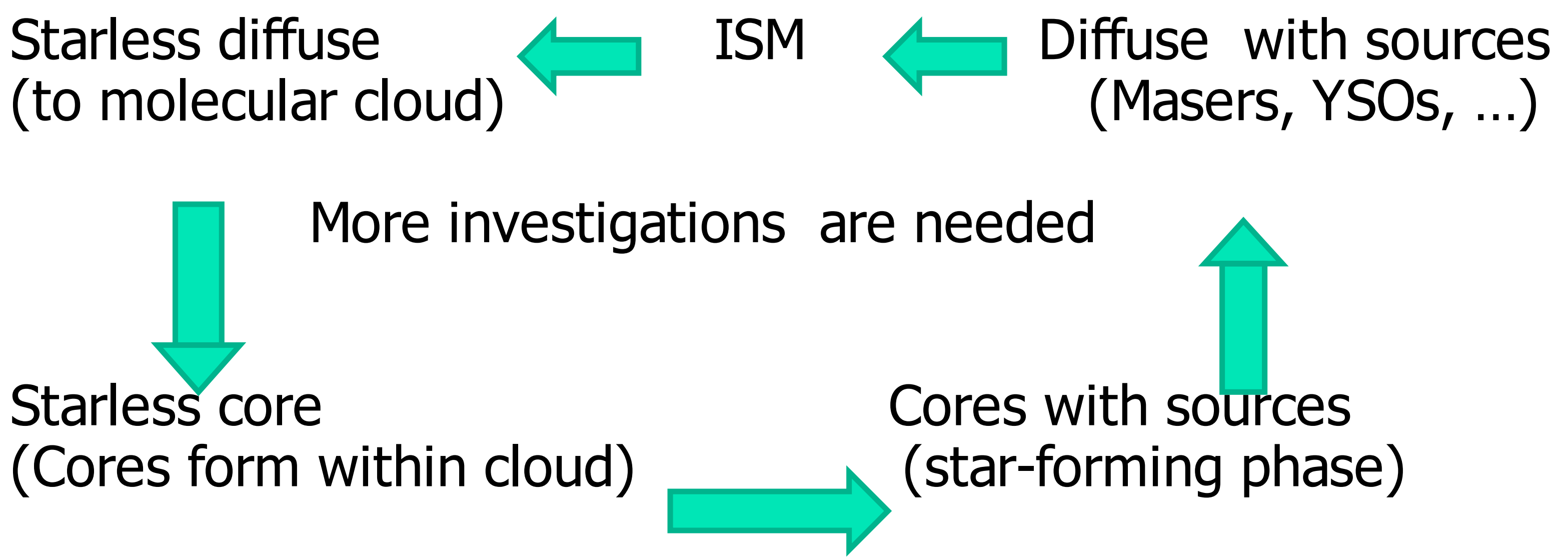

Summary of Millimeter studies and future work:

- 674 clumps/782 cores were surveyed with J=1-0 of 12CO, 13CO and C18O

  Clumps in 4 complexes were mapped
- Gave out the basic parameters of the Planck cold dust cores

  Revealed several results which were not seen before, including:

  --The close agreement of the line center velocity

  --The properties of the distributions of the parameters

  -- the process dynamic at the Galaxy 5 kpc ring

  -- extended the space of the SF region in our Galaxy

  -- closing couple of the gas and dust

  -- the earliest status of the Planck cores
- Further studies: Higher resolution continuum,

  Dense molecular lines; HI line

Thanks to Neal!

Thank you all !